Mathematisches Forschungsinstitut Oberwolfach

Report No. 48/2018

DOI: 10.4171/OWR/2018/48

Computational Engineering

Organised by
Olivier Allix, Cachan
Annalisa Buffa, Lausanne
Carsten Carstensen, Berlin
Joerg Schroeder, Essen

21 October – 27 October 2018

Abstract. This Workshop treated a variety of finite element methods and applications in computational engineering and expanded their mathematical foundation in engineering analysis. Among the 53 participants were mathematicians and engineers with focus on mixed and nonstandard finite element schemes and their applications.

Mathematics Subject Classification (2010): 65K15, 65N15, 65N25, 65N30, 65N50, 65N55, 74B05, 74B20, 74G15, 74S05.

Introduction by the Organisers

This Computational Engineering Workshop covered mathematical and numerical aspects of finite-element methodologies with applications in computational engineering. The presentations established novel methods for various problems next to innovative mathematical aspects of state-of-the-art finite element methods. The presented numerical schemes included mixed finite elements methods, multiscale methods, isogeometric analysis, mapped tent-pitching methods, discontinuous Galerkin methods, discontinuous Petrov-Galerkin methods, stress reconstruction, spectral methods, adaptive methods, hybrid high-order methods, the tangential-displacement normal-normal-stress method, Hodge decomposition methods, local orthogonal decomposition methods, proper generalized decomposition, meshfree methods, and cut finite-element methods. The thirty talks, including an evening session, fostered fruitful discussions between mathematicians and engineers and layed the groundwork for future collaborations in and beyond the context of the Priority Program 1748 “Reliable simulation techniques in solid

mechanics. Development of non-standard discretization methods, mechanical and mathematical analysis" of the German Research Foundation. In particular, the interest and need of DG methods for engineering applications were the focus of discussion within the Engineering community. The Workshop was useful for the engineering community to clarify the differences between the different possible formulations and to address the practical aspect of implementation while opening the mathematical community to challenging problems not properly analyzed so far. The remainder of this report contains the extended abstracts and illustrates the plethora of applications of the abovementioned methods ranging from solid and fluid mechanics to electrodynamics.

Acknowledgement: The MFO and the workshop organizers would like to thank the National Science Foundation for supporting the participation of junior researchers in the workshop by the grant DMS-1049268, "US Junior Oberwolfach Fellows". Moreover, the MFO and the workshop organizers would like to thank the Simons Foundation for supporting Pedro Morin and Thirupathi Gudi in the "Simons Visiting Professors" program at the MFO.

Workshop: Computational Engineering

Table of Contents

Abstracts

Mapped tent pitching methods: explicit methods for hyperbolic systems on unstructured tent meshes

Jay Gopalakrishnan
(joint work with Joachim Schöberl, Christoph Wintersteiger)

Solutions of hyperbolic partial differential equations propagate at finite speed. Hence tent-shaped spacetime regions appear to be natural for solving hyperbolic equations. By constraining the height of the tent pole, one can ensure causality within the tent. This talk will focus on a numerical technique which proceeds by progressively meshing a spacetime domain by tent-shaped objects. The solution can be computed on an unstructured advancing front composed of tent canopies. Such methods are naturally high order in both space and time variables whenever the solution is smooth. The ability to advance in time by different amounts at different spatial locations distinguishes such schemes. We present the history of such techniques and our new additions to improve these schemes. A new twist [1] is to use certain maps, that make fully explicit schemes possible even while using unstructured tents. These degenerate maps transform tents into domains where space and time are separated, thus allowing standard methods to be used within tents. A structure-aware Taylor scheme can be used to perform explicit time stepping within tents.

References

[1] J. Gopalakrishnan, J. Schöberl, and C. Wintersteiger, *Mapped tent pitching schemes for hyperbolic systems*, SIAM Journal on Scientific Computing, 39 (2017), pp. B1043–B1063.

Numerical homogenization of heterogeneous fractional Laplacians

Joscha Gedicke
(joint work with Donald L. Brown, Daniel Peterseim)

In the modeling and simulation of porous media or composite materials, the multiscale nature of the materials is a challenging mathematical problem. In addition, the modeling of non-local behavior that naturally occurs in particular media is of great interest. Therefore, one is interested in the heterogeneous fractional Laplacian model problem:

$$\mathcal{L}_A^s u = f \quad \text{in } \Omega, \qquad \text{and} \qquad u = 0 \quad \text{on } \partial\Omega. \tag{1}$$

This is the Darcy flow model with a multiscale permeability coefficient A and a fractional derivative power $s \in (0, 1)$ to incorporate the non-local behavior.

To efficiently approximate the fractional diffusion problem in heterogeneous media, we employ in [1] the local orthogonal decomposition (LOD) method. The key idea of this multiscale method is to incorporate scales on the fine-grid to the coarse-grid in a computationally feasible way.

It is well known that fractional Laplacian problems are non-local. Therefore, applying standard two-grid techniques to handle heterogeneous coefficients locally is not possible as the sub-grid problems will too be non-local and not decaying exponentially. However, due to the Caffarelli-Silvestre extension [2], one is able to rewrite the non-local fractional Laplacian as a Dirichlet-to-Neumann mapping problem with coefficient y^α in the extended domain $\mathcal{C} = \Omega \times (0, \infty)$:

$$
\begin{aligned}
-\operatorname{div}(y^a B(x) \nabla U) &= 0 \quad \text{in } \mathcal{C}, \\
\frac{\partial U}{\partial \nu^a} = -y^a \frac{\partial U}{\partial y}\bigg|_{y=0} &= c_s f(x) \quad \text{on } \Omega, \\
U &= 0 \quad \text{on } \partial_L \mathcal{C} = \partial\Omega \times [0, \infty).
\end{aligned} \tag{2}
$$

The solution to (1) is then given by $u(x) = U(x, 0)$ for $x \in \Omega$, and the tensor $B \in \mathbb{R}^{d+1} \times \mathbb{R}^{d+1}$ is given by $B(x) = [A(x), 0_{d\times 1}; 0_{1\times d}, 1]$ for $a = 1 - 2s \in (-1, 1)$ or $s = \frac{a-1}{2} \in (0, 1)$. Here, $\frac{\partial U}{\partial \nu^a}$ is the co-normal exterior derivative with outer unit normal ν and $c_s = 2^{1-2s}\frac{\Gamma(1-s)}{\Gamma(s)} > 0$ is a positive constant that solely depends on s. This problem is localizable at the cost of a one dimension higher infinite domain and singular or degenerate coefficients depending on the fractional degree s. To be able to approximate the solution to (2) numerically, we truncate the infinite domain $\mathcal{C}$ to the finite domain $\mathcal{C}_T = \Omega \times (0, T)$ with zero Dirichlet boundary condition at T, cf. [3].

Constructing a quasi-interpolation operator $\mathcal{I}_H$ onto the coarse-scale finite element space V_H with interpolation and stability estimates in y^a-weighted Sobolev norms, and a fine-scale (global) projection operator $Q_{\mathcal{C}_T}$, we are able to apply the LOD method to the extension problem (2). The LOD method leads to the orthogonal decomposition of $\mathring{H}^1_L(\mathcal{C}_T, y^a)$ into a multiscale space $V_H^{ms} = (V_H - Q_{\mathcal{C}}(V_H))$ and a fine scale space $V^f = \{v \in \mathring{H}^1_L(\mathcal{C}_T, y^a) \mid \mathcal{I}_H v = 0\}$, which is the kernel of the quasi-interpolation operator. For the resulting multiscale method, we can prove the following error estimate.

Theorem. *Suppose that $u \in \mathring{H}^1_L(\mathcal{C}_T, y^a)$ is the solution of the truncated extension problem, $u_H^{ms} \in V_H^{ms}$ is the multiscale approximation, and the data is such that $f \in L^2(\Omega)$. Then, we have the following error estimate*

$$\|\nabla u - \nabla u_H^{ms}\|_{L^2(\mathcal{C}_T, y^a)} \lesssim H^s \|f\|_{L^2(\Omega)}.$$

To design a numerically efficient scheme, we show that the approximation of the fine-scale projection operator $Q_{\mathcal{C}_T}$ can be localized, due to the exponential decay of the corrector problems. Utilizing a separate quasi-interpolation on the boundary, we are able to show improved convergence rates. Numerical experiments demonstrate those higher rates and the computational efficiency of the method using local corrector problems.

References

[1] D.L. Brown, J. Gedicke, D. Peterseim, *Numerical homogenization of heterogeneous fractional Laplacians*, Multiscale Model. Simul. **16** (2018), no. 3, 1305–1332.

[2] L. Caffarelli, L. Silvestre, *An extension problem related to the fractional Laplacian*, Comm. Partial Differential Equations, **32** (2007), no. 7-9, 1245–1260.

[3] R.H. Nochetto, E. Otárola, A.J. Salgado, *A PDE approach to fractional diffusion in general domains: a priori error analysis*, Found. Comput. Math. **15** (2015), no. 3, 733–791.

Stress approximation and reconstruction with application to solid mechanics

Fleurianne Bertrand

(joint work with B. Kober, M. Moldenhauer, G. Starke)

Due to the fact that large local stresses are related to failure, accurate stress approximations are of interest in many applications in solid mechanics. In particular, they play an important role in the approximation of surface traction forces.

The finite elements method for elasticity usually consists in minimizing an energy depending on the displacement variable in an appropriate finite element space. An additional pressure variable can be considered such that the approache remain uniformly accurate in the limit of incompressible materials. This leads in general to discontinuous stresses, and the reconstruction of accurate stresses in a localizable post-processing step for elasticity is an ongoing research field see [1, 2]. In the best case, this reconstruction can be build on each element or on vertex-patches, is involving constants depending only of the shape regularity, and remains stable in the incompressible limit. In particular, the asymmetry of such a reconstruction has to be controlled. A further challenging step ist the extension on hyperelastic material models involving geometrical and material nonlinearities.

An alternative approach minimizes a dual energy under the constraints of momentum and leads to an approximation of the stress directly in an $H(div)$ conforming space (see e.g. [3]). This approach is of saddle-point type and the compatibility of the FE spaces has to be proven. In particular, the asymmetry of the stress tensor has to be controlled. To circumvent this restriction, the hyperelasticity problem can be considered directly in the deformed configuration. Here, parametric Raviart-Thomas elements (see [4, 5, 6]) are essential to deal with a domain with curved boundaries.

A third approach consists in the Least-Squares Formulation ([7, 8]). Stress-based variational principles for hyperelastic material models has been studied in [9] using a reference configuration. This work can be extended to a consideration in the actual configuration. The relations between this approach and the stress-based mixed method will be investigated in detail. We aimed to extend the results of [10] to proove that the error associated with the momentum balance and the error between the two stress approximations are of higher order than the overall error for the least-squares approach. Since the Least-Squares Formulation has

an inherent error estimator, this would lead to an error estimator for the mixed approach.

References

[1] F. Bertrand, B. Kober, M. Moldenhauer and G. Starke, *Weakly Symmetric Stress Equilibration and A Posteriori Error Estimation for Linear Elasticity*, submitted, (2018).

[2] F. Bertrand and M. Moldenhauer and G. Starke, *A Posteriori Error Estimation for Planar Linear Elasticity by Stress Reconstruction*, Computational Methods in Applied Mathematics, (2018)

[3] D. Boffi, F. Brezzi and M. Fortin, *Mixed Finite Element Methods and Applications*, Springer, Heidelberg, (1990).

[4] F. Bertrand and G. Starke, *Parametric RT elements for mixed methods on domains with curved surfaces* SIAM J. Numer. Anal., **54** (2016)

[5] F. Bertrand, S. Münzenmaier and G. Starke, *First-order system least squares on curved boundaries: higher-order RT elements*, SIAM J. Numer. Anal., **52**, (2014), 3165–3180.

[6] F. Bertrand, *First-order system least-squares for interface problems*, SIAM J. Numer. Anal., **56**, (2018), 1711–1730.

[7] P. Bochev and M. Gunzburger, *A Locally Conservative Least-Squares Method for Darcy Flows*, Commun. Numer. Meth. Engrg,**24**, 2008, 97–110.

[8] Z. Cai and G. Starke, *Least Squares Methods for Linear Elasticity*, SIAM J. Numer. Anal., **42**, 2004, 826–842.

[9] B. Müller, G. Starke, A. Schwarz and J. Schröder, *A First-Order System Least Squares Method for Hyperelasticity*, SIAM J. Sci. Comput. **36** (2014), B795–B816.

[10] J. Brandts, Y. Chen and J. Yang, *A Note on Least-Squares Mixed Finite Elements in Relation to Standard and Mixed Finite Elements*, IMA J. Numer. Anal. **26** (2006), 779–789.

Model Order Reduction in high-dimensional parameter space

Pierre Ladevèze

(joint work with C. Paillet, D. Néron ; ENS Paris-Saclay)

Model reduction techniques such as Proper Orthogonal Decomposition, Proper Generalized Decomposition and Reduced Basis are decision-making tools which are about to revolutionize many domains. Unfortunately, their calculation remains problematic for problems involving many parameters, for which one can invoke the "curse of dimensionality". The today practical limit is about a dozen parameters and much less for nonlinear engineering problems.

The talk will introduce a general answer to this challenge [1]. This MOR method named the parameter-multiscale PGD is based on the Saint-Venants Principle which works for numerous models in Physics. Such a principle highlights two different levels of parametric influence, which drives us to introduce a multiscale description of the parameters and to separate a macro and a micro scale, as it is classically done for space or time. A first implementation of this vision has been done using a Discontinuous Galerkin spacial formulation and applied to an elasticity 3D-problem composed of up to a thousand parameters. Last developments concern its extension to classical finite element solvers and nonlinear problems [2].

The talk will give the basic features of the parameter-multiscale PGD, especially its mechanical bases, and presents its extensions. Elasticity 3D-problems will be used to illustrate its performance as well as its current limits.The latest developments and perspectives will also be shown.

References

[1] Ladevèze P., Paillet C., Néron D., *Extended-PGD Model Reduction for Nonlinear Solid Mechanics Problems Involving Many Parameters*, (2018). In: Oñate E., Peric D., de Souza Neto E., Chiumenti M. (eds) Advances in Computational Plasticity, Computational Methods in Applied Sciences, **46**, Springer, Cham.

[2] Ladevèze P., *On reduced models in nonlinear solid mechanics*, European Journal of Mechanics A/Solids **60** (2016) 227–237

Sparse Compression of Expected Solution Operators

Daniel Peterseim

(joint work with Michael Feischl)

For a random (or parameterized) family of prototypical linear elliptic partial differential operators $\boldsymbol{\mathcal{A}}(\omega) = -\operatorname{div}(\boldsymbol{A}(\omega)\nabla\bullet)$ and a given deterministic right-hand side f, we consider the family of solutions $\boldsymbol{u}(\omega) := \boldsymbol{\mathcal{A}}(\omega)^{-1}f$ with events $\omega \in \Omega$ in some probability space Ω. We define the harmonically averaged operator

$$\mathcal{A} := \Big(\mathbb{E}[\boldsymbol{\mathcal{A}}(\omega)^{-1}]\Big)^{-1}.$$

The idea behind this definition is that $\mathbb{E}(\boldsymbol{u})$ satisfies $\mathbb{E}[\boldsymbol{u}] = \mathcal{A}^{-1}f$. In this sense, $\mathcal{A}$ may be understood as a stochastically homogenized operator and $\mathcal{A}^{-1}$ is the effective solution operator. Note that this definition does not rely on probabilistic structures of the random diffusion coefficient $\boldsymbol{A}$ such as stationarity, ergodicity or any characteristic length of correlation. However, we shall emphasize that $\mathcal{A}$ does not coincide with the partial differential operator that would result from the standard theory of stochastic homogenization (under stationarity and ergodicity). Recent work on discrete random problems on $\mathbb{Z}^d$ with iid edge conductivies indicates that $\mathcal{A}$ is rather a non-local integral operator [1]. Our paper [2] shows that, even in the more general PDE setup without any assumptions on the distribution of the random coefficient, the expected solution operator $\mathcal{A}^{-1}$ can be represented accurately by a sparse matrices R^δ in the sense that

$$\|\mathcal{A}^{-1} - R^\delta\|_{L^2(D)\to L^2(D)} \leq \delta$$

for any $\delta > 0$ while the number of non-zero entries of R^δ scales like δ^{-d} up to logarithmic-in-δ terms.

The sparse matrix representation of $\mathcal{A}^{-1}$ is based on multiresolution decompositions of the energy space in the spirit of numerical homogenization by localized orthogonal decomposition (LOD) [4, 6, 3] and, in particular, its multi-scale generalization that is popularized under the name gamblets [5]. The gamblet decomposition of [5] is slightly modified by linking it to classical Haar wavelets

via L^2-orthogonal projections and conversely by corrections involving the solution operator. The resulting problem-dependent multiresolution decompositions block-diagonalize the random operator $\boldsymbol{\mathcal{A}}$ for any event in the probability space. The block-diagonal representations (with sparse blocks) are well conditioned and, hence, easily inverted to high accuracy using a few steps of standard linear iterative solvers. The sparsity of the inverted blocks is preserved to the degree that it deteriorates only logarithmically with higher accuracy.

While the sparsity pattern of the inverted block-diagonal operator is independent of the stochastic parameter and, hence, not affected when taking the expectation (or any sample mean) the resulting object cannot be interpreted in a known basis. This issue is circumvented by reinterpreting the approximate inverse stiffness matrices in terms of the deterministic Haar basis before stochastic averaging. This leads to an accurate representation of $\mathcal{A}^{-1}$ in terms of piecewise constant functions. Sparsity is not directly preserved by this transformation but can be retained by some appropriate hyperbolic cross truncation which is justified by scaling properties of the multiresolution decomposition.

Apart from the mathematical question of sparse approximability of the expected operator, the above construction leads to a computationally efficient method for approximating $\mathcal{A}^{-1}$ when combined with any sampling approach for the approximation of the expectation.

For details we refer to [2].

References

[1] J. Bourgain. On a homogenization problem. *Journal of Statistical Physics*, **172-2** (2018), 314–320.

[2] M. Feischl, D. Peterseim, *Sparse compression of expected solution operators*, arXiv preprint **1807.01741** (2018).

[3] R. Kornhuber, D. Peterseim, and H. Yserentant. An analysis of a class of variational multiscale methods based on subspace decomposition. *Math. Comp.*, **87** (2018), 2765–2774.

[4] A. Målqvist, D. Peterseim, *Localization of elliptic multiscale problems*, Mathematics of Computation **83-290** (2014), 2583–2603.

[5] H. Owhadi. Multigrid with rough coefficients and multiresolution operator decomposition from hierarchical information games. *SIAM Review*, **59-1** (2017), 99–149.

[6] D. Peterseim. Variational multiscale stabilization and the exponential decay of fine-scale correctors. In Gabriel R. Barrenechea, Franco Brezzi, Andrea Cangiani, and Emmanuil H. Georgoulis, editors, *Building Bridges: Connections and Challenges in Modern Approaches to Numerical Partial Differential Equations*, Springer (2016), 343–369.

Robust discretization of the Reissner–Mindlin plate with Taylor–Hood FEM

Mira Schedensack
(joint work with D. Gallistl)

The Reissner-Mindlin plate model for a moderately thick plate covering the domain $\Omega \subseteq \mathbb{R}^2$ under a load $f \in L^2(\Omega)$ seeks a displacement $u \in H^1_0(\Omega)$ and a rotation $\phi \in \Phi := H^1_0(\Omega;\mathbb{R}^2)$ with

$$(1)\quad a(\phi,\psi)+t^{-2}(\nabla w-\phi,\nabla v-\psi)_{L^2(\Omega)} = (f,v)_{L^2(\Omega)} \quad \text{for all } (v,\psi)\in H^1_0(\Omega)\times\Phi.$$

Here, $a(\cdot,\cdot)$ is a coercive and continuous bilinear form on Φ, and the thickness t is rescaled by certain material constants. The phenomenon that low-order finite element methods behave poorly for this model when t is small compared to the mesh size, is known as shear locking.

Under the assumption that some $\eta \in H(\operatorname{div},\Omega)$ with $-\operatorname{div}\eta = f$ is known, problem (1) can be reformulated in terms of the gradient, i.e., ∇w (and correspondingly ∇v can be replaced by $\sigma \in Z := \nabla H^1_0(\Omega)$. Furthermore, Z can be characterized via the Helmholtz decomposition as

$$Z = \{\sigma \in [L^2(\Omega)]^2 \mid \forall q \in (H^1(\Omega)\cap L^2_0(\Omega)) : (\sigma, \operatorname{Curl} q)_{L^2(\Omega)} = 0\}.$$

Here, the operator Curl is defined as $\operatorname{Curl} v := (-\partial_2 v, \partial_1 v)^\top$. The work [4] mimics this relation in the discretization, i.e, the discretization of Φ and Z is defined by

$$\Phi_h := [P_{k+2}(\mathcal{T})\cap H^1_0(\Omega)]^2,\ \ X_h := [P_k(\mathcal{T})]^2,\ \ Q_h := P_{k+1}(\mathcal{T})\cap H^1(\Omega)\cap L^2_0(\Omega),$$
$$Z_h := \{\sigma_h \in X_h \mid \forall q_h \in Q_h : (\sigma_h, \operatorname{Curl} q_h)_{L^2(\Omega)} = 0\}.$$

Note that $Z_h \not\subseteq Z$ leads to a nonconforming method. The discrete approximations σ_h and ϕ_h of ∇w and ϕ are then defined by

$$a(\phi_h,\psi_h) + t^{-2}(\sigma_h - \Pi_k\phi_h, \tau_h - \Pi_k\psi_h)_{L^2(\Omega)} = (\eta,\tau_h)_{L^2(\Omega)}$$

with L^2 projection Π_k onto $P_k(\mathcal{T})$.

The definition of Z_h directly implies the discrete Helmholtz decomposition $X_h = Z_h \oplus \operatorname{Curl} Q_h$. With this the discrete problem can be reformulated into a mixed system similar to [1], which then (together with the inf-sup condition of the Taylor–Hood pair (Φ_h, Q_h) [2]) leads to a quasi-optimal error estimate simultaneously in all variables. In this error estimate the error in ϕ is measured in the H^1 norm and the error of $\sigma := \nabla w$ is measured in the L^2 norm. However, in those norms, the discretization spaces Φ_h and X_h are not balanced and this would lead to a suboptimal predicted convergence rate of ϕ. The results of [4] prove that this error

estimate is indeed not sharp in the sense that the error in ϕ can be bounded by

$$|\phi - \phi_h|_{H^1(\Omega)} \leq C \Bigg(\inf_{\psi_h \in \Phi_h} |\phi - \psi_h|_{H^1(\Omega)} + \min \Big\{ \inf_{\beta_h \in Q_h} \big(\|\alpha - \beta_h\|_{L^2(\Omega)} + t\, |\alpha - \beta_h|_{H^1(\Omega)} \big), h^s \inf_{s_h \in Q_h} |p - s_h|_{H^1(\Omega)} + h^s \inf_{\delta_h \in Q_h} |\gamma - \delta_h|_{H^1(\Omega)} + h \|\eta - \Pi_k \eta\|_{L^2(\Omega)} \Big\} \Bigg),$$

where s denotes the elliptic regularity constant from the Poisson-Neumann problem. If all variables are smooth, the first term in the minimum converges with rate $h^{k+2} + th^{k+1}$, while in the asymptotic regime $h \leq t$, the second term in the minimum converges as h^{k+1+s}.

The proposed method is related to those introduced in [1, 3] with the difference that in those works (Φ_h, Q_h) is discretized with a (generalization of) the Mini finite element pair.

References

[1] D.N. Arnold, R.S. Falk, *A uniformly accurate finite element method for the Reissner–Mindlin plate*, SIAM J. Numer. Anal. **26** (1989), 1276–1290.

[2] D. Boffi, *Stability of higher order triangular Hood-Taylor methods for the stationary Stokes equations*, Math. Models Methods Appl. Sci. **4** (1994), 223–235.

[3] D. Gallistl and M. Schedensack, *A robust discretization of the Reissner–Mindlin plate with arbitrary polynomial degree*, submitted (2018).

[4] D. Gallistl and M. Schedensack, *Taylor–Hood discretization of the Reissner–Mindlin plate*, submitted (2018).

DPG for plate problems — traces

Norbert Heuer

(joint work with Thomas Führer, Alexander Haberl, Antti H. Niemi)

The discontinuous Petrov–Galerkin method with optimal test functions (DPG method) is a family of schemes that combine the use of product test spaces with so-called optimal test functions to automatically satisfy the discrete inf-sup condition. In this form it has been proposed by Demkowicz and Gopalakrishnan [1], initially for transport problems. Further advantages of the DPG method are that linear systems have symmetric positive definite matrices, and that it has a built-in a posteriori error estimator.

Practical and theoretical reasons suggest to base DPG approximations on ultraweak variational formulations. In this case, field variables are considered L_2-variables so that test functions carry all the appearing derivatives. Transferring derivatives to test functions by integrating by parts, this gives rise to trace terms and thus, trace operators. In the ultraweak case, trace operators carry all the regularity weight of the problem. They have to be defined in appropriate domain

spaces with corresponding images. Furthermore, whereas discretizations of L_2-field variables are straightforward to implement, discretizations of trace variables are more involved, particularly for problems of higher order.
We discuss strategies and arising difficulties in the case of second and fourth-order operators, specifically for plate problems. Already for the Poisson problem, trace variables live in product spaces, having one component for each element of the mesh. This is due to the fact that test functions are taking from corresponding mesh-related product spaces. There are two natural norms for theses traces, one of quotient space type related to taking traces, and a second one stemming from the duality pairing with test functions of product spaces. It is critical for the DPG analysis (well-posedness and quasi-optimal convergence) that both norms be equivalent.
We motivate the study of trace operators by considering the biharmonic problem. Introducing two variables (the deflection and its Laplacian), an ultraweak formulation generates two trace variables stemming from formally identical integrations by parts. In fact, there are four different possibilities to define related trace operators. We illustrate the effect of different selections with numerical experiments.
As a second problem we consider the Kirchhoff–Love plate bending model with the deflection, rotation (gradient of the deflection) and bending moments as unknowns [2, 3]. In this case, the deflection becomes an L_2-variable by twice integrating by parts. Therefore, the resulting trace operation produces two components. It turns out that in general, these components are not independent. We discuss the exact meaning of this fact, and how the operator can be defined in a well-posed way. Afterwards, we discuss a conforming approximation of this trace variable. In order to be able to use local basis functions (associated with edges and vertices of the mesh) one has to consider a dense subspace of higher regularity. This is similar to the Raviart–Thomas interpolation and the space $\mathrm{H}(\mathrm{div}, T)$ (with element T) where normal boundary traces are usually assumed to be L_2-regular, generating a dense subspace $\mathcal{H}(\mathrm{div}, T) \subset \mathrm{H}(\mathrm{div}, T)$.
As main results we present a well-posed ultraweak formulation of the Kirchhoff–Love model and a quasi-optimally converging fully-discrete DPG scheme. Numerical results confirm expected convergence rates both for quasi-uniform and adaptive mesh refinements.
As a conclusion of the discussion of trace operators in the ultraweak setting we stress the following facts: (i) The regularity of the problem is passed onto the trace variables. (ii) The selections of the domain and test spaces for a trace operator are not necessarily unique but critical for the well-posedness of the formulation. (iii) A stable approximation of trace variables requires to identify components of trace variables that can be separated in a stable way. (iv) In comparison with field variables of corresponding regularity, trace variables are easier to discretize in a conforming way.
Support by CONICYT through FONDECYT projects 1150056 and 11170050 is gratefully acknowledged.

References

[1] L. F. Demkowicz and J. Gopalakrishnan, *A class of discontinuous Petrov-Galerkin methods. Part I: the transport equation*, Comput. Methods Appl. Mech. Engrg. **199** (2010), 1558–1572.

[2] T. Führer, N. Heuer, and A. H. Niemi, *An ultraweak formulation of the Kirchhoff–Love plate bending model and DPG approximation*, Math. Comp., (appeared online, DOI:10.1090/mcom/3381).

[3] T. Führer and N. Heuer, *Fully discrete DPG methods for the Kirchhoff–Love plate bending model*, Comput. Methods Appl. Mech. Engrg. **343** (2019), 550–571.

Hybridizable discontinuous Galerkin formulations with strongly-enforced symmetry of the stress tensor

Antonio Huerta

(joint work with Matteo Giacomini, Ruben Sevilla)

The difficulty of discretizing symmetric second-order tensors in the framework of mixed finite element methods has represented a major limitation to the application of these techniques to engineering problems in computational fluid dynamics and computational solid mechanics for the last 40 years. Owing to its mixed method nature, the hybridizable discontinuous Galerkin (HDG) method is not immune to these issues. A novel HDG formulation exploiting Voigt notation to strongly enforce the symmetry of second-order tensors, by storing solely their non-redundant components, is discussed. When equal polynomials approximations of degree k are used of the primal, $\boldsymbol{u}$, mixed, $\boldsymbol{L}$, and hybrid, $\widehat{\boldsymbol{u}}$, variables, optimal convergence of order $k+1$ is obtained. In particular, this optimal converge of the approximated strain rate tensor $\boldsymbol{L}^h \approx -(\boldsymbol{\nabla u} + \boldsymbol{\nabla u}^T)/2$, being $\boldsymbol{u}$ velocity/displacement field allows to obtain a superconvergent approximation $\boldsymbol{u}^\star$. Namely, for each element $\Omega_e,\ e = 1, \dots, \mathtt{n_{el}}$ by solve

$$\begin{cases} \boldsymbol{\nabla}\cdot\big(\boldsymbol{\nabla}^{\mathrm{S}}\boldsymbol{u}_e^\star\big) = -\boldsymbol{\nabla}\cdot\boldsymbol{L}_e^h & \text{in } \Omega_e, \\ \boldsymbol{n}_e\cdot\boldsymbol{\nabla}^{\mathrm{S}}\boldsymbol{u}_e^\star = -\boldsymbol{n}_e\cdot\boldsymbol{L}_e^h & \text{on } \partial\Omega_e, \end{cases}$$

in the space of polynomials of complete degree at most $k+1$ in each element Ω_e. In order for $\boldsymbol{u}^\star$ to be well-defined, the proposed novel post-processing procedure accounts for both translational and rotational rigid-body motions by means of additional solvability constraints, namely,

$$\int_{\Omega_e} \boldsymbol{u}_e^\star \, d\Omega = \int_{\Omega_e} \boldsymbol{u}_e^h \, d\Omega, \text{ and } \int_{\Omega_e} \boldsymbol{\nabla}\times\boldsymbol{u}_e^\star \, d\Omega = \oint_{\partial\Omega_e} \widehat{\boldsymbol{u}}^h\cdot\boldsymbol{\tau}_e \, d\Gamma.$$

Numerical evidence of optimal convergence and superconvergence in 2D and 3D and for different mesh elements has been provided for both incompressible flow and linear elasticity problems. In the latter, locking-free results are also obtained. Finally, note that also for $k = 0$ optimal convergence is obtained for the primal, mixed, and hybrid variables.

References

[1] R. Sevilla, M. Giacomini, A. Karkoulias and A. Huerta, *A superconvergent hybridisable discontinuous Galerkin method for linear elasticity*, Int. J. Numer. Methods Eng., **116**:2 (2018), 91–116.

[2] M. Giacomini, A. Karkoulias, R. Sevilla and A. Huerta, *A superconvergent HDG method for Stokes flow with strongly enforced symmetry of the stress tensor*, doi: 10.1007/s10915-018-0855-y, J. Sci. Comput. (2018).

[3] R. Sevilla and A. Huerta, *HDG-NEFEM with degree adaptivity for Stokes flows*, doi: 10.1007/s10915-018-0657-2, J. Sci. Comput. (2018).

[4] R. Sevilla, M. Giacomini and A. Huerta, *A face-centred finite volume method for second-order elliptic problems*, Int. J. Numer. Methods Eng., **115**:8 (2018), 986–1014.

Trace Theorems for the Exact Sequence Energy Spaces and Polyhedral Domains

Leszek F. Demkowicz

(joint work with Federico Fuentes)

The presentation was concerned with the classical subject of proving Trace Theorem for the exact sequence energy spaces.

THEOREM 1

Let $s \in (-\frac{1}{2}, \frac{1}{2})$ and let $\Omega \subset \mathbb{R}^3$ be a piece-wise smooth (polyhedral) domain with boundary Γ. There exist three continuous trace operators mapping the differential complex of energy spaces onto *the corresponding trace energy spaces defined on the boundary, and forming a 2D differential complex, with the following commuting diagram.*

$$\begin{array}{ccccc} H^{s+1}(\Omega) & \xrightarrow{\boldsymbol{\nabla}} & H^s(curl,\Omega) & \xrightarrow{\boldsymbol{\nabla}\times} & H^s(div,\Omega) \\ \downarrow \gamma & & \downarrow \gamma_t & & \downarrow \gamma_n \\ H^{s+\frac{1}{2}}(\Gamma) & \xrightarrow{\boldsymbol{\nabla}_\Gamma} & H^{s-\frac{1}{2}}(curl_\Gamma,\Gamma) & \xrightarrow{curl_\Gamma} & H^{s-\frac{1}{2}}(\Gamma) \end{array}$$

∎

Contrary to the original results of A. Buffa, P. Ciarlet, M. Costabel and D. Sheen, [1, 2], construction of the traces follows the classical approach based on the three steps: a) trace theorems for a half-space. b) trace theorems for a hypograph domain. c) trace theorems for a general piece-wise smooth (polyhedral) domain (partition of unity argument).

The ϵ-novelty of the presented results include:

- a unified presentation for the range $s \in (-\frac{1}{2}, \frac{1}{2}$ including density results,
- discussion of minimum-energy extension norms, and
- proofs based on the so-called *Duality Lemma* [3] based on the following elementary observation.

Consider the PDEs resulting from the minimum-energy extension problem for the exact energy spaces:

grad extension:

$$\boldsymbol{\nabla} \cdot (\boldsymbol{\nabla} u) + u = 0\,, \tag{1}$$

curl extension:

$$\boldsymbol{\nabla} \times (\boldsymbol{\nabla} \times E) + E = 0\,, \tag{2}$$

div extension:

$$\boldsymbol{\nabla} (\boldsymbol{\nabla} \cdot v) + v = 0\,. \tag{3}$$

If u solves (1) then $\boldsymbol{\nabla} u$ solves (3). Conversely, if v solves (3) then $\boldsymbol{\nabla} \cdot v$ solves (1). In the same way, if E solves (2) then so does $\boldsymbol{\nabla} \times E$. Moreover, Dirichlet problems are turned into Neumann problems and vice versa.

It turns out that these simple relations allow for (in our opinion) simplified proofs of major results on the subject. For a complete presentation and details, see [4].

References

[1] A. Buffa and P. Ciarlet. On traces for functional spaces related to Maxwell's equations. Part I: an integration by parts formula in Lipschitz polyhedra. Part II: Hodge decompositions on the boundary of Lipschitz polyhedra and applications. *Math. Meth. Appl.*, 21:9–30,31–49, 2001.

[2] A. Buffa, M. Costabel, and D. Sheen. On traces for $H(\mathrm{curl}, \Omega)$ in Lipshitz domains. *J. Math. Anal. Appl.*, 276:845–876, 2002.

[3] C. Carstensen, L. Demkowicz, and J. Gopalakrishnan. Breaking spaces and forms for the DPG method and applications including Maxwell equations. *Comput. Math. Appl.*, 72(3):494–522, 2016.

[4] L. Demkowicz. Lecture notes on Energy Spaces. Technical Report 13, ICES, 2018.

Rayleigh–Ritz approximation of the inf-sup constant for the divergence

Dietmar Gallistl

Let $\Omega \subseteq \mathbb{R}^n$, $n \geq 2$, be a bounded Lipschitz polytope and let $V := H^1_0(\Omega; \mathbb{R}^n)$ denote the space of L^2 vector fields over Ω with generalized first derivatives in $L^2(\Omega)$ and vanishing trace on the boundary, and let $Q := L^2_0(\Omega)$ denote the space of L^2 functions with vanishing average over Ω. It is known [1, 3] that the divergence operator $\mathrm{div} : V \to Q$ possesses a continuous right-inverse, i.e., there exists a positive constant β such that for any $q \in Q$ there exists some $v \in V$ with $\mathrm{div}\, v = q$ and $\beta \|Dv\| \leq \|q\|$ (here $\|\cdot\|$ is the $L^2(\Omega)$ norm). The largest number β with this property is characterized by

$$\beta = \inf_{q \in Q \setminus \{0\}} \sup_{v \in V \setminus \{0\}} \frac{(q, \mathrm{div}\, v)_{L^2(\Omega)}}{\|q\| \|Dv\|}.$$

The numerical approximation of β with stable standard finite element pairings is problematic because convergence cannot be guaranteed in general [2]. Since, with the space of velocity gradients $\Gamma := DV$, the constant β can be rewritten as

$$\beta = \inf_{q \in Q \setminus \{0\}} \sup_{\gamma \in \Gamma \setminus \{0\}} \frac{(q, \operatorname{tr} \gamma)_{L^2(\Omega)}}{\|q\| \|\gamma\|},$$

numerical schemes that directly approximate the space Γ are applicable. The classical Helmholtz decomposition [with $\perp$ denoting L^2 orthogonality in $\Sigma := L^2(\Omega; \mathbb{R}^{n \times n})$] reads

$$\Gamma := \mathfrak{Z}^{\perp}, \quad \text{with } \mathfrak{Z} := [H(\operatorname{div}^0, \Omega)]^n = \{\sigma \in \Sigma : \text{all rows of } \sigma \text{ are divergence-free}\}.$$

The work [5] proposed a discrete analogue in $\Sigma_h := P_k(\mathcal{T}_h; \mathbb{R}^{n \times n})$, the space of piecewise polynomial (of degree $\leq k$) tensor fields with respect to a simplicial triangulation $\mathcal{T}_h$ of Ω, as follows

$$\Gamma_h := \mathfrak{Z}_h^{\perp}, \qquad \text{with } \mathfrak{Z}_h := (RT_k(\mathcal{T}_h)^n \cap \mathfrak{Z}) \subseteq (\mathfrak{Z} \cap \Sigma_h),$$

where $\perp$ denotes L^2 orthogonality in Σ_h and $RT_k(\mathcal{T}_h)^n$ denotes the subspace of Σ whose rows belong to the Raviart–Thomas finite element space. of degree k. The property $\mathfrak{Z}_h \subseteq \Sigma_h$ is well known. One should note that in general $\Gamma_h \not\subseteq \Gamma$.

Let Q_h denote the subspace of Q consisting of $\mathcal{T}_h$-piecewise polynomial functions of degree $\leq k$. The approximation β_h is defined as

$$\beta_h = \inf_{q_h \in Q_h \setminus \{0\}} \sup_{\gamma_h \in \Gamma_h \setminus \{0\}} \frac{(q_h, \operatorname{tr} \gamma_h)_{L^2(\Omega)}}{\|q_h\| \|\gamma_h\|}.$$

For the convergence analysis, the following equivalent formulation of the problem turns out useful. It is well known [2] that

$$\beta^2 = \inf_{v \neq 0} \frac{\|\operatorname{div} v\|^2}{\|Dv\|^2} \tag{1}$$

where the infimum is taken over the V-orthogonal complement (that is, with respect to the inner product $(D\cdot, D\cdot)_{L^2(\Omega)}$) of the divergence-free functions in V.

Theorem [4]. *Let $(\mathcal{T}_h)_h$ be a sequence of nested partitions such that the mesh size function h uniformly converges to zero. Then the sequence $(\beta_h)_h$ converges monotonically from above towards the inf-sup constant β, i.e.,*

$$\beta_h \searrow \beta \quad \textit{under mesh refinement.}$$

Provided that the square of the inf-sup constant β^2 is an eigenvalue of (1) with normalized eigenfunction $u \in H^{1+s}(\Omega; \mathbb{R}^n)$ for some $0 < s < \infty$, then for small h the following error bound holds

$$\frac{\beta_h^2 - \beta^2}{\beta^2} \leq C \|h\|_{L^\infty(\Omega)}^{2r} \|u\|_{H^{1+s}(\Omega)}^2$$

for the rate $r := \min\{k+1, s\}$ and some mesh-size independent constant $C > 0$.

References

[1] G. Acosta, R. G. Durán, M. A. Muschietti, *Solutions of the divergence operator on John domains*, Adv. Math., **206** no. 2 (2006), 373–401.

[2] C. Bernardi, M. Costabel, M. Dauge, V. Girault, *Continuity properties of the inf-sup constant for the divergence*, SIAM J. Math. Anal., **48** no. 2 (2016), 1250–1271.

[3] M. E. Bogovskiĭ, *Solution of the first boundary value problem for an equation of continuity of an incompressible medium*, Dokl. Akad. Nauk SSSR, **248** no. 5 (1979), 1037–1040.

[4] D. Gallistl, *Rayleigh–Ritz approximation of the inf-sup constant for the divergence*, Math. Comp. **88** no. 315 (2019), 73–89.

[5] M. Schedensack, *A new generalization of the P_1 non-conforming FEM to higher polynomial degrees*, Comput. Methods Appl. Math., **17** no. 1 (2017), 161–185.

Finite element methods for nonsmooth problems and application to a problem in optimal insulation

Sören Bartels

Given a hot metal ball and a small amount of insulation material how should one arrange an insulating film on the surface of the ball so that the heat inside the ball is conserved as long as possible? This question can be reformulated as a minimization of the principal eigenvalue of the partial differential operator related to the Laplace operator with Robin-type boundary condition, i.e., the operator $\mathcal{A}_\ell$ related to the boundary value problem

$$-\Delta u = f \text{ in } \Omega, \quad \ell\, \partial_n u + u = 0 \text{ on } \partial\Omega.$$

Here, $\ell : \partial\Omega \to [0,\infty)$ is a function that defines the thickness of the insulating film. The eigenvalue λ_m is determined by minimizing a Rayleigh quotient, i.e.,

$$\lambda_\ell = \min_{\|u\|_{L^2(\Omega)}=1} \|\nabla u\|^2 + \int_{\partial\Omega} \ell^{-1} u^2 \,\mathrm{d}s.$$

Minimizing the eigenvalue over insulating films ℓ of fixed total mass $m > 0$ leads after an exchange of the order of minimization and elimination of ℓ to the nonlinear eigenvalue problem

$$\lambda_m = \min_{\|\ell\|_{L^1(\partial\Omega)}=m} \lambda_\ell = \min_{\|u\|_{L^2(\Omega)}=1} \|\nabla u\|^2 + m^{-1}\Big(\int_{\partial\Omega} |u| \,\mathrm{d}s\Big)^2.$$

For an optimal nonnegative eigenfunction u_m the optimal insulating film is proportional to the trace of u, i.e., $\ell(s) = m u_m(s)/\|u_m\|_{L^1(\partial\Omega)}$. By comparing the eigenvalue λ_m to the smallest nontrivial Dirichlet and Neumann eigenvalues of the Laplace operator one observes a surprising break of symmetry.

Theorem ([3])**.** *Let $\Omega = B_r(0)$ be a ball of radius $r > 0$. There exists a constant $m_0 > 0$ such that for every $0 < m < m_0$ eigenfunctions u_m are nonradial. In particular, corresponding optimal films have gaps, i.e., the zero set of every optimal film ℓ has positive Hausdorff measure on $\partial\Omega$.*

The proof of this result is nonconstructive and does not provide information about the geometry and regularity of the insulating film ℓ. To reliably approximate

optimal films we numerically solve the nonsmooth eigenvalue problem defining λ_m. For this, we apply techniques recently developed for the approximation of nonsmooth variational problems, in particular for problems involving the total variation. An important model problem is the related gradient or subdifferential flow which is formally given by

$$\partial_t u = \operatorname{div} \frac{\nabla u}{|\nabla u|}, \quad u(0) = u^0.$$

A natural discretization uses the backward difference quotient operator $d_t a^k = (a^k - a^{k-1})/\tau$ for a step-size $\tau > 0$, a regularization of the modulus and a semi-implicit treatment of the nonlinear term, i.e., we compute a sequence $(u^k)_{k=0,1,\dots} \subset H^1(\Omega)$ via the recursion

$$d_t u^k = \operatorname{div} \frac{\nabla u^k}{|\nabla u^{k-1}|_\varepsilon}.$$

Here, e.g., $|a|_\varepsilon = (a^2 + \varepsilon^2)^{1/2}$ for some $\varepsilon > 0$. A recent result in [2] shows that this iteration is unconditionally energy stable in the sense that

$$\mathrm{TV}_\varepsilon(u^K) + \tau \sum_{k=1}^{K} \|d_t u^k\|^2_{L^2(\Omega)} \le \mathrm{TV}_\varepsilon(u^0), \quad \mathrm{TV}_\varepsilon(u) = \int_\Omega |\nabla u|_\varepsilon \mathrm{d}x.$$

holds for all $K \ge 0$. This unexpected result is a consequence of certain delay properties of discrete quotient and product rules, e.g., $d_t(1/c_k) = -d_t c^k/(c^{k-1}c^k)$. The regularization and the semi-implicit treatment do not lead to stability restrictions but affect the approximation properties, we refer the reader to [2] for details.

We also use a gradient flow to determine the eigenvalue λ_m, i.e., using the L^2 scalar product $(\cdot,\cdot)$ we define a sequence of functions $(u^k)_{k=0,1,\dots} \subset H^1(\Omega)$ via

$$(d_t u^k, v) + (\nabla u^k, \nabla v) + m^{-1}\|u^{k-1}\|_{L^1(\partial\Omega)} \int_{\partial\Omega} \frac{u^k v}{|u^{k-1}|_\varepsilon} \,\mathrm{d}s = 0$$

for all $v \in H^1(\Omega)$ subject to the linearized normalization conditions $(d_t u^k, u^{k-1}) = 0$ and $(v, u^{k-1}) = 0$. The iteration is stable under mild conditions and provides accurate approximations of λ_m, see [1]. Numerical experiments reported therein show that optimal insulating films are continuous leaving a gap on one side of a ball and have maximal thickness on the opposite side.

References

[1] S. Bartels, G. Buttazzo, *Numerical solution of a nonlinear eigenvalue arising in optimal insulation*, Interfaces Free Bound. (to appear), arXiv:1708.03762 (2017).

[2] S. Bartels, L. Diening, R.H. Nochetto, *Unconditional stability of semi-implicit discretizations of singular flows*, SIAM J. Numer. Anal. **53** (3) (2018), 1896–1914.

[3] D. Bucur, G. Buttazzo, C. Nitsch, *Symmetry breaking for a problem in optimal insulation*, J. Math. Pures Appl., **107** (4) (2017), 451–463.

Efficient spectral methods for nonlinear Hamiltonian systems

Zhimin Zhang
(joint work with Jing An, Waixiang Cao)

Hamiltonian dynamical systems have applications in classical mechanics, molecular dynamics, hydrodynamics, electrodynamics, plasma physics, relativity, astronomy, and other scientific fields [16, 17]. However, for most nonlinear Hamiltonian systems, it is impossible to find exact solutions and efficient numerical methods are desired. On the other hand, a Hamiltonian system has some remarkable properties, most important among which are its symplectic structure and energy preservation. A good numerical scheme should be able to mimic as many of these physical properties as possible.

The symplectic geometry algorithm that maintains the symplectic structure for Hamiltonian systems appeared in literature as early as 1984 by Feng [6]. Since then symplectic algorithms have been intensively studied. We refer to [7, 8, 9, 10, 14, 20] for an incomplete list of references. However, none of the symplectic algorithms are energy-preserving. In fact, it was proved in [5, 24] that there exists no energy-preserving symplectic algorithm for general nonlinear Hamiltonian systems. On the other hand, it is well known that Galerkin-type methods such as finite element methods preserve energy. Then we face a dilemma and have to choose between preserving energy and preserving symplectic structure. Many scholars pointed out that preserving energy may be more important than the symplectic structure for highly oscillatory problems [14, 22, 2, 19].

In the last decade, much insight into the properties of energy conservation for Hamiltonian systems has also been gained. In [23], Chen et al. used finite element methods to solve ordinary differential equations and proved that the linear element was a second-order pseudo-symplectic scheme, the quadratic element was a third-order pseudo-symplectic scheme, respectively, and both linear and quadratic elements preserved energy. However, to predict orbital evolution, linear and quadratic finite elements require a tremendous amount of computation, and accumulation of round-off errors will be eventually dominant. Other numerical methods have been proposed in the literature to study the long-time energy conservation. In [1], Cohen used a modulated Fourier expansion to show long-time near-conservation of the total and oscillatory energies for Hamiltonian systems with highly oscillatory solutions. In a more recent work [13], Hairer and Lubich studied the long-time behavior of the Störmer-Verlet-leapfrog method for highly oscillatory Hamiltonian systems with a slowly varying, solution-dependent high frequency, and proved that the proposed method conserved approximately a modified total energy over a long time interval. We also refer to [3, 12] for some more works in this direction. In the spirit of high-order methods, Kanyamee and Zhang [18], Huang and Zhang [15] proposed algorithms based upon the spectral collocation method to preserve both energy and volume (symplectic structure) up to numerically negligible errors. Numerical evidence demonstrated their algorithms are energy and volume preserving in practice. This approach, although is lack of

theoretical analysis, works well for some problems, especially in simulating long time behavior. The drawback is that the differential matrices are usually full and the condition number of the stiffness matrix increases dramatically with increasing polynomial degrees. Large condition numbers lead to instability of the algorithm in some situations, e.g., the calculation of many-body problems.

The main purpose of the current work is to present and study a class of efficient high accuracy polynomial spectral methods that preserve the energy and symplectic structure simultaneously in practice (with numerically neglectable errors) for nonlinear Hamiltonian systems. By "spectral" we mean the convergence is achieved by increasing polynomial degrees rather than decreasing the step-size in time (as most of ODE and Hamiltonian solvers in the literature). Different from earlier works [18] and [15] in this direction, we provide rigorous mathematical analysis to show the high-order accuracy (actually spectral accuracy under reasonable assumptions) of these spectral methods, as well as energy and symplectic structure conservation. To be more precise, we present three polynomial spectral methods: spectral Petrov-Galerkin method (which is not discussed in the literature for Hamiltonian systems), spectral Gauss collocation method (which has been used before), and spectral Galerkin method, and prove that they share the same property of high-order (spectral) rate of convergence and are capable of long time simulation. Furthermore, we investigate properties of symplectic structure and energy conservation for the three numerical methods and establish theoretical results including:

(1) The Petrov-Galerkin method preserves the energy exactly and spectral Galerkin method is energy conserving up to spectral accuracy.

(2) Both spectral Galerkin and Petrov-Galerkin methods are symplectic up to spectral accuracy.

(3) Both spectral Galerkin and Petrov-Galerkin methods converge with exponential rate under analytic regularity assumption, which most Hamiltonian system satisfy.

In other words, our methods not only preserve the energy, but also preserve symplectic structure with numerically negligible error in practice, due to the spectral accuracy. We observe (theoretically and numerically) that the proposed spectral methods have many desirable properties and are more efficient than existing symplectic methods and low-order finite element methods. Moreover, the stiff matrices of Petrov-Galerkin and spectral Galerkin methods are both sparse and hence well conditioned. In order to overcome the large condition number problem of the spectral Gauss collocation method [18], we propose a preconditioning technique, which yields a sparse and well conditioned stiff matrix.

We would like to indicate that the Gauss collocation method is a well-known symplectic scheme (see, e.g., [14]) and the spectral Gauss collocation method has been used to solve some ordinary differential equations (see, e.g., [11]) and its conservation of energy up to a numerical quadrature error was mentioned in [18]. However, we have not found any rigorous mathematical proof of energy conservation property for spectral Gauss collocation methods when applied to Hamiltonian

systems. Furthermore, to the best of our knowledge, there is no any study of symplectic and energy conservation for the Petrov-Galerkin method in this context, and therefore, our spectral Petrov-Galerkin method is a new method for solving Hamiltonian dynamical systems.

In numerical simulation, we separate the gradient of the Hamiltonian to linear and nonlinear parts, and use implicit scheme for the linear part and explicit scheme for the non-linear part. Numerical test data demonstrate that this approach works very efficiently and the time accumulation of the error is linear. Comparing with existing symplectic methods and low-order Galerkin methods, our theoretical and numerical results have demonstrated that spectral methods have some desirable properties and advantages.

1. They are high-order methods with spectral accuracy and hence require less CPU time than traditional methods to achieve the same accuracy.
2. They preserve energy and symplectic structure in practice for some reasonable polynomial degree N.
3. They predict more accurate trajectories in long-time.

The ability to simulate long-time behavior of Hamiltonian systems makes the three spectral methods more appealing for solving partial different equations with high-order derivatives.

References

[1] D. Cohen, *Conservation properties of numerical integrators for highly oscillatory Hamiltonian systems*, IMA J. Numer. Anal. **26** (2006), 34–59.

[2] D. Cohen, E. Hairer, and C. Lubich, *Conservation of energy, momentum and actions in numerical discretizations of nonlinear wave equations*, Numer. Math. **110** (2008), 113–143.

[3] P. Console, E. Hairer, and C. Lubich, *Symmetric multistep methods for constrained Hamiltonian systems,* Numer. Math. **124** (2013), 517–539.

[4] P.J. Davis and P. Rabinowitz, Methods of Numerical Integration, Courier Corporation, 2007.

[5] E. Faou, E. Hairer, and T.L. Pham, *conservation with non-symplectic methods: examples and counter-examples.* BIT Numer. Math. **44** (2004), 699–709.

[6] K. Feng, *On difference schemes and symplectic geometry*, In: Proceedings of the 5th International Symposium on Differential Geometry and Differential Equations, 1984.

[7] K. Feng, *Difference schemes for Hamiltonian formalism and symplectic geometry*, J. Comput. Math. **4** (1986), 279–289.

[8] K. Feng and M. Qin, *Symplectic Geometric Algorithms for Hamiltonian Systems*, Springer, Berlin, 2010.

[9] K. Feng and M. Qin, *The symplectic methods for the computation of Hamiltonian equations*, In: Numerical Methods for Partial Differential Equations, Springer, Berlin, Heidelberg, 1987, 1–37.

[10] K. Feng, H. Wu, M. Qin, and D. Wang, *Construction of canonical difference schemes for Hamiltonian formalism via generating functions*, J. Comput. Math. **7** (1989), 71–96.

[11] B.-Y. Guo and Q.-Z. Wang, *Legendre-Gauss collocation methods for ordinary differential equations*, Adv. Comput. Math., **30** (2009), 249–280.

[12] E. Hairer and C. Lubich, *Long-time energy conservation of numerical methods for oscillatory differential equations*, SIAM J. Numer. Anal. **38** (2000), 414–441.

[13] E. Hairer and C. Lubich, *Long-term analysis of the Störmer-Verlet method for Hamiltonian systems with a solution-dependent high frequency*, Numer. Math. **134** (2016), 119–138.

[14] E. Hairer, C. Lubich and G. Wanner, Geometric Numerical Integration. Structure-Preserving Algorithms for Ordinary Differential Equations, 2nd ed., Springer Science in Computational Mathematics 31, Springer-Verlag, Berlin, 2006.
[15] C. Huang and Z. Zhang, *Spectral collocation method for differential algebraic equations with arbitrary index: with application to Hamiltonian systems*, J. Sci. Comput. **58** (2014), 499–516.
[16] J.E. Marsden, G. Misiolek, J.P. Ortega, M. Perlmutter, and T.S. Ratiu, Hamiltonian Reduction by Stages, Springer, 2007.
[17] J.E. Marsden and M. West, *Discrete mechanics and variational integrators*, Acta Numerica **10** (2001), 357–514.
[18] K. Nanyamee and Z. Zhang, *Comparison of a spectral collocation method and symplectic methods for Hamilton systems,* International Journal of Numerical Analysis and Modeling **8** (2011), 86–104.
[19] J.M. Sanz-Serna, *Symplectic integrators for Hamiltonian problems: an overview*, Acta Numerica **1** (1992), 243=-286.
[20] J.M. Sanz-Serna and M.P. Calvo, Numerical Hamiltonian Problems, Courier Dover Publications, 2018.
[21] J. Shen, T. Tang, and L.-L. Wang, Spectral Methods: Algorithms, Analysis and Applications, Springer Science and Business Media, 2011.
[22] A. Stuart and A. R. Humphries, Dynamical Systems and Numerical Analysis, Cambridge University Press, 1998.
[23] Q. Tang, C. Chen, and L. Liu, *Energy conservation and symplectic properties of continuous finite element methods for Hamiltonian systems*, Applied Mathematics and Computation **181** (2006), 357–1368.
[24] G. Zhong and J.E. Marsden, *Lie-Piosson Himilton-Jacobi theory and Lie-Poisson integrators*, Phys. Lett. A. **133** (1988), 134–139.

Weakly symmetric stress methods for elasto-plasticity

Gerhard Starke

The extension of stress-based mixed finite element methods based on the Hellinger-Reissner variational principle to elasto-plastic deformations is investigated in this contribution. Historically, the treatment of elasto-plasticity was one of the motivations for the use of stress-based methods as can be read in one the earliest such contributions [ABD84]: "the elimination of the stresses from the equilibrium and constitutive equations of a material exhibiting plastic behaviour is difficult; consequently, only a mixed formulation is feasible." Our aim is to use weakly symmetric stress approximations, in particular, starting from the finite element combination by Boffi, Brezzi and Fortin [BBF09]. For the problem of linear elasticity, this method consists in finding $\boldsymbol{\sigma}_h \in \boldsymbol{\Sigma}_h$, $\mathbf{u}_h \in \mathbf{V}_h$ and $\boldsymbol{\rho}_h \in \mathbf{R}_h$ such that

$$\begin{aligned} (\mathcal{A}(\boldsymbol{\sigma}^N + \boldsymbol{\sigma}_h), \boldsymbol{\tau}_h) + (\mathbf{u}_h, \operatorname{div} \boldsymbol{\tau}_h) + (\boldsymbol{\rho}_h, \mathbf{as}\, \boldsymbol{\tau}_h) &= 0\,, \\ (\operatorname{div}(\boldsymbol{\sigma}^N + \boldsymbol{\sigma}_h) + \mathbf{f}, \mathbf{v}_h) &= 0\,, \\ (\mathbf{as}\,(\boldsymbol{\sigma}^N + \boldsymbol{\sigma}_h), \boldsymbol{\theta}_h) &= 0 \end{aligned} \tag{1}$$

holds for all $\boldsymbol{\tau}_h \in \boldsymbol{\Sigma}_h$, $\mathbf{v}_h \in \mathbf{V}_h$ and $\boldsymbol{\rho}_h \in \mathbf{R}_h$ holds. The finite element spaces $\boldsymbol{\Sigma}_h \in H_{\Gamma_N}(\operatorname{div}, \Omega)^d$, $\mathbf{V}_h \in L^2(\Omega)^d$, $\mathbf{R}_h \in L^2(\Omega)^{d\times d,\mathrm{as}}$ may be chosen as next-to-lowest order Raviart-Thomas elements (RT_1^d), piecewise linear functions (DP_1^d),

and skew-symmetric matrices with piecewise linear continuous entries ($P_1^{d\times d,\mathrm{as}}$). Here, $\mathcal{A}$ represents the stress-to-strain map from linear elasticity given by

$$\mathcal{A}\boldsymbol{\tau} = \frac{1}{2\mu}\left(\boldsymbol{\tau} - \frac{\lambda}{3\lambda+2\mu}(\operatorname{tr}\boldsymbol{\tau})\mathbf{I}\right)$$

with Lamé parameters λ, μ. The surface tractions prescribed on Γ_N are built into $\boldsymbol{\sigma}^N \in H(\operatorname{div},\Omega)$ and volume forces are given by $\mathbf{f}$.

For the treatment of elasto-plastic material behaviour based on a von Mises flow rule, the stresses are restricted further by the inequality constraint $|\mathbf{dev}\,\boldsymbol{\sigma}_h| \le \kappa$, for the deviatoric, i.e., trace-free, stress component. It is also a time-dependent, although quasi-static, problem which is realized, for example, by a steady increase of the surface traction $\boldsymbol{\sigma}^N(t)\cdot\mathbf{n} = \ell(t)$ on Γ_N. The (discrete) admissible set of stresses is therefore given by

$$\begin{aligned}\mathcal{K}_{\ell(t)} =\{&\boldsymbol{\sigma}_h \in \boldsymbol{\sigma}^N(t) + \boldsymbol{\Sigma}_h : (\operatorname{div}\boldsymbol{\sigma}_h + \mathbf{f}, \mathbf{v}_h) = 0 \text{ for all } \mathbf{v}_h \in \mathbf{V}_h\,,\\ &(\mathbf{as}\,\boldsymbol{\sigma}_h, \boldsymbol{\theta}_h) = 0 \text{ for all } \boldsymbol{\theta}_h \in \mathbf{R}_h\,,\ (|\mathbf{dev}\,\boldsymbol{\sigma}_h| - \kappa, \omega_h) \le 0 \text{ for all } \omega_h \in X_h^+\}\end{aligned}$$

for some appropriate subset of nonnegative functions X_h^+ of some finite element space. The saddle-point problem (1) is replaced by the time-dependent variational inequality of finding $\boldsymbol{\sigma}_h(t) \in \mathcal{K}_{\ell(t)}$ such that

$$(\mathcal{A}\dot{\boldsymbol{\sigma}}_h(t), \boldsymbol{\tau}_h - \boldsymbol{\sigma}_h) \ge 0 \text{ holds for all } \boldsymbol{\tau}_h \in \mathcal{K}_0$$

(cf. [HR13, Sect. 8.1]). The incremental formulation determines, based on the approximation $\boldsymbol{\sigma}^{\mathrm{old}}$ from the previous time-step, $\boldsymbol{\sigma}_h(t) \in \mathcal{K}_{\ell(t)}$ such that

$$(\mathcal{A}(\boldsymbol{\sigma}_h(t) - \boldsymbol{\sigma}^{\mathrm{old}}), \boldsymbol{\tau}_h - \boldsymbol{\sigma}_h) \ge 0 \text{ holds for all } \boldsymbol{\tau}_h \in \mathcal{K}_0\,. \tag{2}$$

We treat this variational inequality by a semi-smooth Newton method which results in a primal-dual active set strategy (cf. [HIK03]) and investigate the resulting linearized problems for inf-sup stability. In the perfectly plastic case (κ constant) in two space dimensions, it turns out that the stress space $\boldsymbol{\Sigma}_h$ needs to be augmented with non-conforming bubbles of the form $\boldsymbol{\nabla}^\perp \mathbf{B}_3^{\mathrm{nc}}$, where $\mathbf{B}_3^{\mathrm{nc}}$ denotes the space of (component-wise) piecewise cubic functions such that $\langle \mathbf{b}, \mathbf{q}\rangle_E = 0$ for all $\mathbf{q} \in P_1(E)^2$ on all edges E of the triangulation. This results in a non-symmetric version of the symmetric stress space studied in [GG11]. In the case of elasto-plasticity with hardening, the original stress-space from the linear elasticity case can be used.

References

[ABD84] D. N. Arnold, F. Brezzi, and J. Douglas, *PEERS: A new mixed finite element for plane elasticity*, Japan J. Appl. Math. **1** (1984), 347–367.

[BBF09] D. Boffi, F. Brezzi, and M. Fortin, *Reduced symmetry elements in linear elasticity*, Commun. Pure Appl. Anal. **8** (2009), 95–121.

[GG11] J. Gopalakrishnan and J. Guzmán, *Symmetric nonconforming mixed finite elements for linear elasticity*, SIAM J. Numer. Anal. **49** (2011), 1504–1520.

[HIK03] M. Hintermüller, K. Ito, and K. Kunisch. *The primal-dual active set strategy as a semismooth Newton method*, SIAM J. Optim. **13** (2003), 865–888.

[HR13] W. Han and B. D. Reddy, *Plasticity: Mathematical Theory and Numerical Analysis*, Springer, New York, 2nd edition, 2013.

Tangential Displacement Normal Normal Stress (TDNNS) Continuous Mixed Finite Elements - New Estimates and Applications in Nonlinear Elasticity

Joachim Schöberl

The TDNNS mixed finite element methods uses tangentially continuous Nedelec finite elements for the displacement variable, and normal-normal continuous symmetric-matrix valued finite elements for the stress variable. The proper spaces for such elements are $H(\mathrm{curl})$ and $H(\mathrm{div}\,\mathrm{div}) = \{\sigma \in L_2^{d\times d,\mathrm{sym}} : \mathrm{div}\,\mathrm{div} \in H^{-1}\}$. We present new estimates in discrete norms mimicking this spaces. We discuss a corresponding discretization for Reissner Mindlin plate models. As the thickness-parameter t tends to 0, the finite element solution converges to the solution obtained by the classical Hellan-Hermann-Johnson method.

We present the extension to geometrically non-linear shells, and to elastodynamics. Here, the displacement is discretized in $(H^1)^d$, but the velocity in $H(\mathrm{curl})$.

Toward Predictive Models of Tumor Growth

J. Tinsley Oden

(joint work with Ernesto A. B. F. Lima, Barbara Wolhmuth, Marvin Fritz, Alican Ozkan, Neda Ghousifam , Nichole Rylander, Tom Yankeelov, and David Fuentes)

This talk begins with a brief review of the conceptual, mathematical, and statistical properties of models necessary for meaningful prediction of physical events in the presence of uncertainties. A Bayesian framework for model calibration, selection, and validation is described that is implemented using the OPAL algorithm, described in previous work.

The microenvironment of multicell tumors at the tissue scale is described with reference to various key cell types, extra-cellular matrix, matrix-degenerative enzymes and other constituents. A general model of such systems based on continuum mixture theory and the Weinberg-Hanahan hallmarks of cancers is presented. Principal unknowns are the volume fractions of cell species. Constitutive equations governing mass flux, mass sources, mechanical deformation and velocity are presented, the latter following a Darcy-Forchheimer-Brinkman law. By introducing a general form of the Ginsberg-Landau energy involving volume fractions of multiple cell species and their gradients, a large family of models of tumor growth is obtained, including reaction-diffusion and phase-field models with and without mechanical deformations. In addition, three models of radiation therapy are introduced. In total, 39 possible tumor growth models are generated within this framework, all with multiple non-deterministic parameters.

Applications of the OPAL algorithm for model section, calibration, and validation are described for laboratory tests with murine models (laboratory rats) injected with glioma cancer cells, with data on the subsequent growth of cancer maintained by MRI images collected every two days over a 20-24-day period with radiation applied around two weeks in the experiments. It is demonstrated that the most plausible valid tumor growth models among this class of models can be identified for given accuracy tolerances and that quite accurate predictions of tumor volume or mass can be obtained by the models passing the OPAL criteria for predictability.

Other *in vitro* experiments for model calibration are mentioned that involve carefully orchestrated tests of liver cell lines growing in specifically-designed laboratory environments. This data is used to calibrate phase-field models of tumor growth. Validation tests on liver cancer using data obtained at M.D. Anderson Cancer Center are planned for future work on these classes of models.

Discontinuous Skeletal Methods for the Obstacle Problem

Thirupathi Gudi
(joint work with Alexandre Ern, Matteo Cicuttin)

Let $\Omega \subset \mathbb{R}^d (2 \leq d \leq 3)$ be a bounded polyhedral domain with boundary $\partial\Omega$. Suppose that $f \in L^2(\Omega)$, $\chi \in H^1(\Omega) \cap C(\bar{\Omega})$ and $g \in H^{1/2}(\partial\Omega)$ are given such that $\chi \leq g$ on $\partial\Omega$. Define $\mathcal{K} := \{v \in H^1(\Omega) : v \geq \chi \text{ a.e. in } \Omega,\ v = g\}$. The elliptic obstacle problem is to find $u \in \mathcal{K}$ such that

$$(\nabla u, \nabla(v - v)) \geq (f, v - u) \quad \forall v \in \mathcal{K},$$

where $(\cdot, \cdot)$ denotes the $L^2(\Omega)$ inner-product for both scalar and vector valued functions. Let $\mathcal{T}_h$ denote the partition of Ω into polyhedral meshes with matching interfaces. The set of cell interfaces in $\mathcal{T}_h$ is denoted by $\mathcal{F}_h$. Let $k \in \{0, 1\}$. The global discrete space is defined by

$$U_h^k := \big(\times_{T \in \mathcal{T}_h} \mathbb{P}_d^0(T) \big) \times \big(\times_{F \in \mathcal{F}_h} \mathbb{P}_{d-1}^k(F) \big).$$

For all $T \in \mathcal{T}_h$, we define the local space $U_T^k := \mathbb{P}_d^0(T) \times \big(\times_{F \in \mathcal{F}_T} \mathbb{P}_{d-1}^k(F) \big)$, here $\mathcal{F}_T$ denotes the set of all faces on ∂T. We define the local reconstruction operator $p_T^{k+1} : U_T^k \to \mathbb{P}_d^{k+1}(T)$ so that, for all $v_h = (v_T, v_{\partial T}) \in U_T^k$,

$$(\nabla p_T^{k+1}(v_h), \nabla w)_T = (\nabla v_T, \nabla w)_T + (v_{\partial T} - v_T, \nabla w \cdot n_T)_{\partial T} \quad \forall w \in \mathbb{P}_d^{k+1}(T),$$
$$(p_T^{k+1}(v_h), 1)_T = (v_T, 1)_T.$$

Let π_T^0 be the L^2-projection onto $\mathbb{P}_d^0(T)$ and let $\pi_{\partial T}^k$ be the L^2-projection onto $\mathbb{P}_{d-1}^k(\partial T)$. We define the local stabilization operator $S_{\partial T}^k : U_T^k \to \mathbb{P}_{d-1}^k(\partial T)$ such that, for all $v_h = (v_T, v_{\partial T}) \in U_T^k$, we have

$$S_{\partial T}^k(v_h) := \pi_{\partial T}^k \big(v_{\partial T} - p_T^{k+1}(v_h) \big) - \pi_T^0 \big(v_T - p_T^{k+1}(v_h) \big)_{|\partial T}.$$

We define the local discrete bilinear form $a_T : U_T^k \times U_T^k \to \mathbb{R}$ by

$$a_T(w_h, v_h) := (\nabla p_T^{k+1}(w_h), \nabla p_T^{k+1}(v_h))_T + (\eta_{\partial T} S_{\partial T}^k(w_h), S_{\partial T}^k(v_h))_{\partial T},$$

with the piecewise constant weight $\eta_{\partial T}$ defined on ∂T such that $\eta_{\partial T|F} = h_F^{-1}$ for all $F \in \mathcal{F}_T$. The global discrete bilinear form a_h on $U_h^k \times U_h^k$ is defined by

$$a_h(w_h, v_h) := \sum_{T \in \mathcal{T}_h} a_T(w_h, v_h) + \sum_{F \in \mathcal{F}_h^b} a_{F^b}(w_{T(F)}, v_{T(F)}),$$

with the Nitsche-type boundary penalty bilinear form

$$\begin{aligned} a_{F^b}(w_{T(F)}, v_{T(F)}) := &-(\nabla p_{T(F)}^{k+1}(w_{T(F)}) \cdot n_\Omega, v_F)_F - (w_F, \nabla p_{T(F)}^{k+1}(v_{T(F)}) \cdot n_\Omega)_F \\ &+ \varsigma h_F^{-1}(w_F, v_F)_F, \end{aligned}$$

where $\varsigma > 0$ is the boundary penalty parameter and n_Ω is the unit outward normal to Ω. Here $\mathcal{F}^b$ denotes the set of faces on $\partial\Omega$ and for $F \in \mathcal{F}^b$, $T(F)$ is the cell sharing the face F. The linear form ℓ_h on U_h^k is defined by

$$\ell_h(v_h) := \sum_{T \in \mathcal{T}_h} (f, v_T)_T - (g, \nabla p_{T(F)}^{k+1}(v_{T(F)}) \cdot n_\Omega)_F + \varsigma h_F^{-1}(g, v_F)_F.$$

The discrete admissible set $\mathcal{K}_h^k$ is defined by

$$\mathcal{K}_h^k := \left\{ v_h \in U_h^k : (v_T, 1)_T \geq (\chi, 1)_T, \ \forall T \in \mathcal{T}_h \right\}.$$

The discrete elliptic obstacle problem consists of finding $u_h \in \mathcal{K}_h^k$ such that

$$a_h(u_h, v_h - u_h) \geq \ell_h(v_h - u_h) \qquad \forall v_h \in \mathcal{K}_h^k.$$

The following theorem establishes energy norm error estimates of order 1 for $k = 0$, and of order $3/2 - \epsilon$ for $k = 1$.

Theorem. If $k = 1$, let $\epsilon \in (0, \frac{1}{2}]$, set $r = \frac{3}{2} - \epsilon$, and assume that $u \in H^{1+r}(D) = H^{\frac{5}{2}-\epsilon}(D)$, $(u - \chi) \in W^{2+\frac{1}{p}-\frac{\epsilon}{2},p}(D)$ with $p = \frac{2(d-1)}{\epsilon} \in (1, \infty)$, and $\lambda := -f - \Delta u \in W^{1-\epsilon,1}(D)$. If $k = 0$, set $r = 1$, let $\tau \in (0, 1)$, and assume that $u \in H^{1+r}(D) = H^2(D)$, $(u - \chi) \in W^{2,p}(D)$ with $p = \frac{d}{\tau} \in (1, \infty)$, and $\lambda := -f - \Delta u \in W^{\tau,1}(D)$. Then, there is C, uniform with respect to h, such that the following holds true:

$$\left(\sum_{T \in \mathcal{T}_h} \|\nabla(u - p_T^{k+1}(u_h))\|_T^2 + \sum_{F \in \mathcal{F}_h^b} h_F^{-1} \|u - u_F\|_F^2 \right)^{\frac{1}{2}} \leq C\big(|u|_{H^{1+r}(D)} + \Phi_{u,\lambda}\big) h^r.$$

where

$$\Phi_{u,\lambda} = \begin{cases} \|u - \chi\|_{W^{2+\frac{1}{p}-\frac{\epsilon}{2},p}(D)}^{\frac{1}{2}} |\lambda|_{W^{1-\epsilon,1}(D)}^{\frac{1}{2}} & \text{if } k = 1, \\ \|u - \chi\|_{W^{2,p}(D)}^{\frac{1}{2}} |\lambda|_{W^{\tau,1}(D)}^{\frac{1}{2}} & \text{if } k = 0. \end{cases}$$

References

[1] M. Cicuttin, A. Ern, T. Gudi, *Discontinuous skeletal methods for lienar and quadratic reconstructios for the elliptic obstacle problem*, HAL preprint, HAL id: hal-01718883.

Hodge decomposition methods for electromagnetics

Li-yeng Sung
(joint work with S.C. Brenner, J. Cui, J. Gedicke, Z. Nan, J. Sun)

Let $\Omega \subset \mathbb{R}^2$ be a bounded polygonal domain. The Hodge decomposition (cf. [6]) of a vector field $\boldsymbol{u} \in H(\mathrm{div}^0;\Omega)$ is given by

$$\boldsymbol{u} = \mathrm{curl}\,\phi + \sum_{j=1}^{m} c_j \,\mathrm{grad}\,\varphi_j \tag{1}$$

where $\phi \in H^1(\Omega)$ has zero mean, $m+1$ equals the number of the components of $\partial\Omega$, $c_1,\ldots,c_m$ are constants, and $\varphi_1,\ldots,\varphi_m$ are harmonic functions such that φ_i equals 1 on the i-th inner component of $\partial\Omega$ and vanishes at all the other components of $\partial\Omega$.

For the Maxwell equations with the perfectly conducting boundary condition

$$\mathrm{curl}\,(\mathrm{curl}\,\boldsymbol{u}) + \alpha\boldsymbol{u} = \boldsymbol{f} \quad \text{in } \Omega \tag{2a}$$

$$\mathrm{div}\,\boldsymbol{u} = 0 \quad \text{in } \Omega \tag{2b}$$

$$\boldsymbol{n} \times \boldsymbol{u} = 0 \quad \text{on } \partial\Omega \tag{2c}$$

where α is not a Maxwell eigenvalue, the idea of the Hodge decomposition approach is to find $\boldsymbol{u}$ by obtaining the function ϕ and the coefficients $c_1,\ldots,c_m$ in (1).

First we find $\xi = \mathrm{curl}\,\boldsymbol{u} \in H^1(\Omega)$ with zero mean that satisfies

$$(\mathrm{curl}\,\xi, \mathrm{curl}\,\psi) + \alpha(\xi,\psi) = (\boldsymbol{f}, \mathrm{curl}\,\psi) \qquad \forall\,\psi \in H^1(\Omega) \tag{3}$$

where $(\cdot,\cdot)$ is the inner product of $L_2(\Omega)$. Then we determine $\phi \in H^1(\Omega)$ with zero mean by

$$(\mathrm{curl}\,\phi, \mathrm{curl}\,\psi) = (\xi,\psi) \qquad \forall\,\psi \in H^1(\Omega) \tag{4}$$

If Ω is not simply connected (and hence $\alpha \neq 0$), we can find $c_1,\ldots,c_m$ by solving the $m \times m$ system

$$\sum_{j=1}^{m} (\mathrm{grad}\,\varphi_j, \mathrm{grad}\,\varphi_k) c_j = \frac{1}{\alpha}(\boldsymbol{f}, \mathrm{grad}\,\varphi_k) \qquad \text{for } 1 \le k \le m \tag{5}$$

Finally we recover $\boldsymbol{u}$ through (1).

This procedure converts the boundary value problem (2) for the Maxwell equations into standard second order scalar elliptic boundary value problems (3)–(5) that can be solved by many numerical schemes (cf. [1, 2]).

The Hodge decomposition approach can also be applied to the general time-harmonic Maxwell equations

$$\mathrm{curl}\,(\mu^{-1}\mathrm{curl}\,\boldsymbol{u}) - k^2\epsilon\boldsymbol{u} = \boldsymbol{f} \qquad \text{in } \Omega$$

$$\mathrm{div}\,(\epsilon\boldsymbol{u}) = 0 \qquad \text{in } \Omega$$

with general boundary conditions (cf. [3, 4]).

Application of the Hodge decomposition approach to a boundary value problem involving the operator curl^4 can be found in [5].

References

[1] S.C. Brenner, J. Cui, Z. Nan, and L.-Y. Sung. Hodge decomposition for divergence-free vector fields and two-dimensional Maxwell's equations. *Math. Comp.*, 81:643–659, 2012.

[2] S.C. Brenner, J. Gedicke, and L.-Y. Sung. An adaptive P_1 finite element method for two-dimensional Maxwell's equations. *J. Sci. Comput.*, 55:738–754, 2013.

[3] S.C. Brenner, J. Gedicke, and L.-Y. Sung. An adaptive P_1 finite element method for two-dimensional transverse magnetic time harmonic Maxwell's equations with general material properties and general boundary conditions. *J. Sci. Comp.*, 68:848–863, 2016.

[4] S.C. Brenner, J. Gedicke, and L.-Y. Sung. Hodge decomposition for two-dimensional time-harmonic Maxwell's equation: impedance boundary condition. *Math. Methods Appl. Sci.*, 40:370–390, 2017.

[5] S.C. Brenner, J. Sun, and L.-Y. Sung. Hodge decomposition methods for a quad-curl problem on planar domains. *J. Sci. Comput.*, 73:495–513, 2017.

[6] V. Girault and P.-A. Raviart. *Finite Element Methods for Navier-Stokes Equations. Theory and Algorithms.* Springer-Verlag, Berlin, 1986.

Surrogate model of a random two-phase material using Gaussian Random Field of Matérn covariance

Barbara Wohlmuth

(joint work with J. Tinsley Oden, Ustim Khristenko)

We are interested in a fast technique for generating synthetic samples of a random two-phase composite, given only a small number of original samples of the real material (e.g. tomography image). For this purpose, we aim to construct an appropriate surrogate model. We define our surrogate phase field as in [1, 2, 3] through the level-cut of some intensity field $u(\underline{x};\omega)$:

$$\chi(\underline{x};\omega) = \begin{cases} 1, & \text{if } u(\underline{x};\omega) \geq \tau, \qquad \text{inclusions} \\ 0, & \text{if } u(\underline{x};\omega) < \tau, \qquad \text{matrix} \end{cases}$$

$\omega \in \Omega$ – a suitable sample space, where the level τ controls the volume fractions of inclusions. We consider the intensity $u(\underline{x})$ as a zero-mean Gaussian random field with covariance of Matérn class, that is of the form

$$\mathcal{C}(\underline{x},\underline{y}) = \frac{\sigma^2}{2^{\nu-1}\Gamma(\nu)} \, (\sqrt{2\nu}\, r)^{\nu} \, \mathcal{K}_{\nu}(\sqrt{2\nu}\, r), \qquad r = \sqrt{(\underline{x}-\underline{y})\underline{\underline{\Theta}}^{-1}(\underline{x}-\underline{y})},$$

with unit standard deviation $\sigma = 1$, where Γ and $\mathcal{K}_{\nu}$ denote the Euler Gamma function and the modified Bessel function of the second kind, respectively. The scalar parameter $\nu > 0$ defines differentiability (smoothness) of the field, while the second order tensor $\underline{\underline{\Theta}}$ defines the shape of inclusions [5]. In particular, $\underline{\underline{\Theta}} = \ell^2 \, \underline{\underline{\mathrm{Id}}}$ corresponds to an isotropic covariance with correlation length ℓ.

It was shown in [4] that $u(\underline{x};\omega)$ solves a fractional SPDE in $\mathbb{R}^d$, $d \in \mathbb{N}$, namely,

$$\left(\mathrm{Id} - \frac{1}{2\nu} \nabla \cdot (\underline{\underline{\Theta}} \, \nabla) \right)^{\frac{1}{2}(\nu + \frac{d}{2})} u(\underline{x};\omega) = \eta \, \dot{\mathcal{W}}(\underline{x};\omega),$$

where $\dot{\mathcal{W}}$ is a spacial white noise in $\mathbb{R}^d$, and η is a normalization coefficient:

$$\eta^2 = \frac{(4\pi)^{\frac{d}{2}} \, |\underline{\underline{\Theta}}|^{\frac{1}{2}} \, \Gamma(\nu + d/2)}{(2\nu)^{\frac{d}{2}} \, \Gamma(\nu)}.$$

This equation is solved by using a Fast Fourier Transform on an extended domain [6], which leads to fast sampling of the phase field $\chi(\underline{x}, \omega)$.

Such a surrogate material is entirely described by the design parameters ν, $\underline{\underline{\Theta}}$ and τ, which control smoothness, shape and volume fraction of inclusions, respectively. In the isotropic case $\underline{\underline{\Theta}} = \ell^2 \, \underline{\underline{\mathrm{Id}}}$, a mapping from a real material to the design parameter space (ν, ℓ, τ) can be constructed using the first two moments of the random field $\chi(\underline{x}, \omega)$:

$$S_1 = \phi = \frac{1}{2\pi} \int_\tau^\infty e^{-\frac{1}{2}t^2} \, \mathrm{d}t, \tag{1}$$

$$S_2(\underline{x}, \underline{y}) = \frac{1}{2\pi} \int_0^{\mathcal{C}(\underline{x},\underline{y})} e^{-\frac{\tau^2}{1+t}} \frac{\mathrm{d}t}{\sqrt{1-t^2}} + \phi^2, \tag{2}$$

where ϕ is the expectation of the volume fraction of the inclusions. From (1), the parameter τ is uniquely defined through the given volume fraction expectation ϕ:

$$\tau = \sqrt{2} \, \mathrm{erf}^{-1}(1 - 2\phi),$$

where $\mathrm{erf}(x)$ denotes the Gauss error function. Then, the parameters ν and ℓ can be approximated using nonlinear least squares regression to fit the real material covariance (original image autocorrelation) with the surrogate covariance (2).

Having now a construction algorithm for samples at hand, we can easily evaluate statistical properties for different quantities of interest in a given material class.

References

[1] S. Torquato, *Random heterogeneous materials: microstructure and macroscopic properties.*

[2] N.F. Berk, *Scattering properties of the leveled-wave model of random morphologies*, Physical Review A **44** (1991), 5069-5079.

[3] M. Teubner, *Level surfaces of Gaussian random fields and microemulsions*, Europhysics Letters **14** (1991), 403–408.

[4] P. Whittle, *On stationary processes in the plane*, Biometrika (1954), 434–449.

[5] L. Roininen, J.M.J. Huttunen, S. Lasanen, *Whittle-Matérn priors for Bayesian statistical inversion with applications in electrical impedance tomography*, Inverse Probl. Imaging **8** (2014), 561–586.

[6] U. Khristenko, L. Scarabosio, P. Swierczynski, E. Ullmann, B. Wohlmuth, *Analysis of boundary effects on PDE-based sampling of Whittle-Matérn random fields*, arXiv:1809.07570 (2018).

Multivariate Adaptive Splines: Theory and Applications

Bert Jüttler

The mathematical technology of tensor-product NURBS (Non-Uniform Rational B-spline) forms the basis for the representations of shapes in Computer Aided Geometric Design [8] and for numerical simulation via Isogeometric Analysis (IGA) [4]. However, this technology does not provide the possibility of adaptive refinement, a feature which is highly useful for geometric modeling and strongly desired in numerical simulation. In order to overcome this limitation, several generalizations of tensor-product NURBS representations have been proposed. These include T-splines, locally refined B-splines, and hierarchical B-splines.

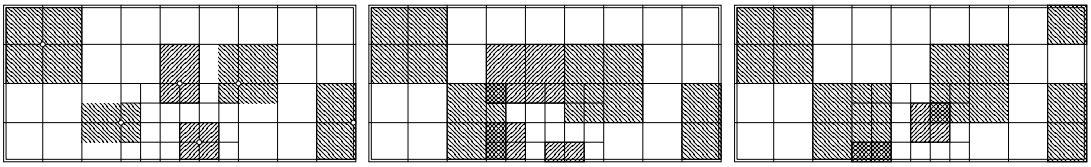

Figure 1. Bilinear T-, LR and hierarchical B-splines on a T-mesh.

T-splines were introduced in 2003 by Sederberg et al. [16]. Their construction is based on a box mesh with hanging nodes, which is used to derive a collection of tensor-product B-splines with individual knot vectors. The original construction does not guarantee the linear independence of the blending functions. Analysis-suitable T-splines, which were also characterized as dual compatible T-splines, impose certain restrictions on the underlying meshes that imply this property [2, 14]. A refinement algorithm with optimal complexity, which creates nested sequences of spline spaces, was studied in [15]. Starting with the two articles [1, 6], T-splines found numerous applications for adaptive numerical simulation.

Locally Refined (LR) B-splines were established in 2013 by Dokken et al. [5]. The constructions starts from the set of B-splines defined by the standard tensor product of univariate spline bases. The associated regular grid is then refined by inserting mesh-line segments. This triggers the subdivision of the B-splines whose support is split by the segment. Repeated insertions define the set of LR B-splines on the resulting box partition of the domain, which are a collection of weighted tensor-product B-splines that form a convex partition of unity. The set of LR B-splines is independent of the order of the mesh-line segment insertions. The construction implies that LR B-spline refinement generates nested spline spaces, but linear independence is not always guaranteed. Applications of LR B-splines to adaptive numerical simulation were reported in [12]. Hierarchical mesh refinement allows to achieve linear independence and algebraic completeness [3].

The hierarchical refinement of B-splines was first described by Forsey and Bartels [9]. Nine years later, Kraft established a selection mechanism that generates a basis of the associated spline space [13]. The construction is based on sequences of nested spline spaces and inversely nested subdomains. A B-spline is selected for inclusion into the basis if its support is contained in the associated subdomain

but not in the next finer one. Starting with [17], hierarchical splines are now frequently used for adaptive numerical simulation in IGA. Another basis, which was introduced in 2012 [10], restores the partition of unity by suitable modifying the basis functions. More precisely, its construction is based on a truncation mechanism, which eliminates the contributions of functions that are selected at higher levels. This provides substantial advantages for geometric design and numerical simulation [11]. Generalizations of hierarchical splines to non-nested sequences of domains have been studied recently, in order to increase the flexibility of the refinement algorithms [7].

References

[1] Y. Bazilevs et al., *Isogeometric analysis using T-splines*, Comp. Meth. Appl. Mech. Engrg. **199** (2010), 229–263.

[2] L. Beirão da Veiga, A. Buffa, D. Cho, and G. Sangalli. *Analysis-suitable T-splines are dual-compatible*, Comp. Meth. Appl. Mech. Engrg. **249-252** (2012), 42–51.

[3] A. Bressan, B. Jüttler, *A hierarchical construction of LR meshes in 2D*, Comp. Aided Geom. Des. **37** (2015), 9-24.

[4] J.A. Cottrell, T.J.R. Hughes, Y. Bazilevs, *Isogeometric analysis: Toward Integration of CAD and FEA*, Wiley, 2009.

[5] T. Dokken, T. Lyche, K.F. Pettersen, *Polynomial splines over locally refined box partitions*, Comp. Aided Geom. Des. **30** (2012), 331-356.

[6] M. Dörfel, B. Jüttler, B. Simeon. *Adaptive isogeometric analysis by local h-refinement with T-splines*, Comp. Meth. Appl. Mech. Engrg. **199** (2010), 264–275.

[7] N. Engleitner, B. Jüttler, *Patchwork B-spline refinement*, Comp.-Aided Des. **90** (2017), 168-179.

[8] G. Farin, J. Hoschek, M.-S. Kim, *Handbook of Computer Aided Geometric Design*, Elsevier, 2002.

[9] D.R. Forsey and R.H. Bartels, Hierarchical B-spline refinement, *Computer Graphics* **22** (1988), 205-212.

[10] C. Giannelli, B. Jüttler, H. Speleers, *THB-splines: The truncated basis for hierarchical splines*, Comp. Aided Geom. Des. **29** (2012), 485-498.

[11] C. Giannelli et al., *THB-splines: An effective mathematical technology for adaptive refinement in geometric design and isogeometric analysis*, Comp. Meth. Appl. Mech. Engrg. **299** (2016), 485-498.

[12] K.A. Johannesen, T. Kvamsdal, T. Dokken, *Isogeometric Analysis using LR B-splines*, Comp. Meth. Appl. Mech. Engrg. **269** (2014), 471-514.

[13] R. Kraft, *Adaptive and linearly independent multilevel Bsplines*, in: A. Le Méhauté et al. (eds.), *Surface Fitting and Multiresolution Methods*, Vanderbilt University Press, Nashville, 1997, 209-218.

[14] X. Li, J. Zheng, T.W. Sederberg, T.J.R. Hughes, and M.A. Scott. *On linear independence of T–spline blending functions*, Comp. Aided Geom. Des. **29** (2012), 63–76.

[15] P. Morgenstern D. Peterseim, *Analysis-suitable adaptive T-mesh refinement with linear complexity*, Comp. Aided Geom. Des. **34** (2015), 50–66.

[16] T.W. Sederberg, J. Zheng, A. Bakenov, A. Nasri. *T-splines and T-NURCCS*, ACM Transactions on Graphics **22** (2003), 477–484.

[17] A.-V. Vuong, C. Giannelli, B. Jüttler, B. Simeon, *A hierarchical approach to adaptive local refinement in isogeometric analysis*, Comput. Methods Appl. Mech. Engrg. **200** (2011), 3554-3567.

A consistent and scalable meshfree mimetic method for conservation laws

Pavel Bochev
(joint work with Nat Trask, Mauro Perego)

Mimetic PDE discretizations utilize the generalized Stokes theorem to construct compatible grad, div and curl operators. However, meshfree methods lack innate notions of cells, faces and edges that facilitate such a construction, causing a dearth of truly compatible meshfree discretizations. In this work, we formulate an abstract mimetic meshfree divergence (MMD) operator that satisfies a discrete divergence theorem and is first-order accurate. Let X be a point cloud representing a bounded region $\Omega \in \mathbb{R}^d$, $d = 2, 3$. We assume that all cloud points on Γ are centroids of boundary segments Γ_i. Let $\chi_i(\Gamma) = \Gamma_i$ if $\boldsymbol{x}_i \in \Gamma$ and $\chi_i(\Gamma) = \emptyset$ otherwise. Let $\boldsymbol{u}^h$ denote a vector field sampled on X. We define the abstract MMD operator as

$$(DIV\boldsymbol{u}^h)_i := \frac{1}{\mu_i}\left[\sum_{\boldsymbol{f}_{ij}\in\partial\omega_i} \boldsymbol{t}_{ij}^{\intercal}(\boldsymbol{u}^h)\,\boldsymbol{\mu}_{ij} + \int_{\chi_i(\Gamma)} \boldsymbol{u}\cdot\boldsymbol{n}dS\right] \quad \forall\omega_i \tag{1}$$

where ω_i is a virtual cell corresponding to $\boldsymbol{x}_i \in X$ with volume μ_i , $\boldsymbol{\mu}_{ij} \in \mathbb{R}^{n_f}$ is a vector of moments assigned to virtual face $\boldsymbol{f}_{ij}$, and $\boldsymbol{t}_{ij}(\boldsymbol{u}^h) \in \mathbb{R}^{n_f}$ is a set of field moments matching the face moments.

We consider two instantiations of (1). The first one assumes a background mesh and uses generalized moving least squares (GMLS) to obtain the necessary field and face moments. This MMD instance is appropriate for settings where mesh is available but its quality is insufficient for a robust and accurate mesh-based discretization. The second instance retains the GMLS field moments and uses the ε_g-ball graph $G_{\varepsilon_g}(V, E)$ of X, with vertices $V = X$ and edges E as a surrogate primal mesh. We assign a virtual dual cell and face to every vertex and edge in this graph to obtain a virtual dual mesh. Assuming a quasi-uniform point cloud we set $\mu_i = |\Omega|/|X|$. To obtain the face moments we require that (1) holds for all linear vector fields and seek $\boldsymbol{\mu}_{ij}$ in terms of scalar potentials. This gives rise to a computationally efficient weighted graph-Laplacian problems for the potentials. The second MMD instance does not require a background grid and is appropriate for applications where quality mesh generation is problematic and/or computationally expensive. Such a discretization allows one to trade a potentially challenging mesh generation problem for a scalable algebraic one, without sacrificing compatibility with the divergence operator. We demonstrate the approach by using the MMD operator to obtain a virtual finite-volume discretization of conservation laws on point clouds. Numerical results confirm the mimetic properties of the method and show that it behaves similarly to standard finite volume methods.

Acknowledgments

This work was supported by the U.S. Department of Energy, Office of Science, Office of Advanced Scientific Computing Research, and the Laboratory Directed Research and Development program at Sandia National Laboratories. Sandia National Laboratories is a multimission laboratory managed and operated by National Technology and Engineering Solutions of Sandia, LLC., a wholly owned subsidiary of Honeywell International, Inc., for the U.S. Department of Energy's National Nuclear Security Administration under contract DE-NA-0003525. SAND2018-12413 A.

A Priori Error Control of DGFEM for the Von Kármán Equations

Neela Nataraj

(joint work with Carsten Carstensen, Gouranga Mallik)

The article concerns discontinuous Galerkin finite element methods (DGFEM) for the approximation of regular solution to the von Kármán equations defined on a polygonal bounded Lipschitz domain $\Omega \subset \mathbb{R}^2$, that describe the deflection of very thin elastic plates. Those plates are modeled by a semi-linear system of fourth-order partial differential equations and described as: for a given load function $f \in L^2(\Omega)$, seek u, v such that

$$(1) \quad \Delta^2 u = [u, v] + f \text{ and } \Delta^2 v = -\frac{1}{2}[u, u] \text{ in } \Omega, u = \frac{\partial u}{\partial \nu} = v = \frac{\partial v}{\partial \nu} = 0 \text{ on } \partial\Omega$$

with $\Delta^2 \varphi := \varphi_{xxxx} + 2\varphi_{xxyy} + \varphi_{yyyy}$, and $[\eta, \chi] := \eta_{xx}\chi_{yy} + \eta_{yy}\chi_{xx} - 2\eta_{xy}\chi_{xy}$.

Nonconforming FEMs have been analyzed for this problem in [1], *a priori* error analysis for a C^0 interior penalty method is studied in [2] and the results of this article are published in [3]. Under minimal regularity assumption of the exact solution, optimal order *a priori* error estimates are obtained for a DGFEM and a novel C^0 interior penalty method is recovered. The *a priori* analysis in [2] controls the error in a stronger norm and is more involved.

The weak formulation for (1) seeks $u, v \in X := H_0^2(\Omega)$ such that for all $\varphi_1, \varphi_2 \in X$,

$$(2) \quad a(u, \varphi_1) + b(u, v, \varphi_1) + b(v, u, \varphi_1) = (f, \varphi_1), \quad a(v, \varphi_2) - b(u, u, \varphi_2) = 0.$$

Here, $a(\eta, \chi) := \int_\Omega D^2\eta : D^2\chi \, \mathrm{dx}$, and $b(\eta, \chi, \varphi) := -\frac{1}{2}\int_\Omega [\eta, \chi]\varphi \, \mathrm{dx}$ for all $\eta, \chi, \varphi \in X$. The vector form seeks $\Psi = (u, v) \in \boldsymbol{X} := X \times X$ such that

$$(3) \quad N(\Psi; \Phi) := A(\Psi, \Phi) + B(\Psi, \Psi, \Phi) - L(\Phi) = 0 \text{ for all } \Phi \in \boldsymbol{X},$$

where for all $\Xi = (\xi_1, \xi_2), \Theta = (\theta_1, \theta_2)$, and $\Phi = (\varphi_1, \varphi_2) \in \boldsymbol{X}$, $L(\Phi) := (f, \varphi_1)$, $A(\Theta, \Phi) := a(\theta_1, \varphi_1) + a(\theta_2, \varphi_2)$, and $B(\Xi, \Theta, \Phi) := b(\xi_1, \theta_2, \varphi_1) + b(\xi_2, \theta_1, \varphi_1) - b(\xi_1, \theta_1, \varphi_2)$. Let $|||\bullet|||_2$ denote the product norm on $\boldsymbol{X}$ defined by $|||\Phi|||_2 := (|\varphi_1|^2_{2,\Omega} + |\varphi_2|^2_{2,\Omega})^{1/2}$ for all $\Phi = (\varphi_1, \varphi_2) \in \boldsymbol{X}$. The approximation of a regular solution Ψ to the non-linear operator $N(\Psi; \Phi) = 0$ for all $\Phi \in \boldsymbol{X}$ of (3) is considered in the sense that the bounded derivative $DN(\Psi)$ of the operator N at the solution Ψ is an isomorphism in the Banach space.

Let $\mathcal{T}$ be a shape-regular triangulation of the domain into closed triangles with set of edges $\mathcal{E}$. Define $h_{\mathcal{T}}(x) = h_K = \operatorname{diam}(K)$ for all $x \in K$, $K \in \mathcal{T}$, and set $h := \max_{K\in\mathcal{T}} h_K$ (resp. $h_{\mathcal{E}}|_E = h_E = \operatorname{diam}(E)$ for any $E \in \mathcal{E}$). Let $P_r(K)$ denote the set of all polynomials of degree less than or equal to r and $P_r(\mathcal{T}) := \big\{\varphi \in L^2(\Omega) : \forall K \in \mathcal{T}, \varphi|_K \in P_r(K)\big\}$ and write $\boldsymbol{P}_r(\mathcal{T}) := P_r(\mathcal{T}) \times P_r(\mathcal{T})$. The jump $[\varphi]_E$ and the average $\langle\varphi\rangle_E$ across the edges E follows the standard definition. For any vector function, jump and average are understood componentwise. For $1/2 < \alpha \leq 1$, let $Y_h := (X \cap H^{2+\alpha}(\Omega)) + P_2(\mathcal{T})$ and $\boldsymbol{Y}_h := Y_h \times Y_h$. For all $\eta, \chi \in Y_h$, $\varphi \in X + P_2(\mathcal{T})$, let $l_{\mathrm{dG}}(\varphi) := \sum_{K\in\mathcal{T}} \int_K f\varphi \,\mathrm{dx}$,
$a_{\mathrm{dG}}(\eta,\chi) := \sum_{K\in\mathcal{T}} \int_K D^2\eta : D^2\chi \,\mathrm{dx} - (J(\eta,\chi) + J(\chi,\eta)) + J_{\sigma_1,\sigma_2}(\eta,\chi)$; $\sigma_1, \sigma_2 > 0$
$b_{\mathrm{dG}}(\eta,\chi,\varphi) := -\frac{1}{2}\sum_{K\in\mathcal{T}} \int_K [\eta,\chi]\varphi \,\mathrm{dx}$,
$J(\eta,\chi) = \sum_{E\in\mathcal{E}} \int_E [\nabla\chi]_E \cdot \langle D^2\eta\, \nu_E\rangle_E \,\mathrm{ds}$, and
$J_{\sigma_1,\sigma_2}(\eta,\chi) := \sum_{E\in\mathcal{E}} \frac{\sigma_1}{h_E^3} \int_E [\eta]_E[\chi]_E \,\mathrm{ds} + \sum_{E\in\mathcal{E}} \frac{\sigma_2}{h_E} \int_E [\nabla\eta\cdot\nu_E]_E[\nabla\chi\cdot\nu_E]_E \,\mathrm{ds}$.
The DGFEM of (1) seeks $(u_{\mathrm{dG}}, v_{\mathrm{dG}}) \in \boldsymbol{P}_2(\mathcal{T})$ such that, for all $(\varphi_1,\varphi_2) \in \boldsymbol{P}_2(\mathcal{T})$,
$a_{\mathrm{dG}}(u_{\mathrm{dG}},\varphi_1) + b_{\mathrm{dG}}(u_{\mathrm{dG}}, v_{\mathrm{dG}}, \varphi_1) + b_{\mathrm{dG}}(v_{\mathrm{dG}}, u_{\mathrm{dG}}, \varphi_1) = l_{\mathrm{dG}}(\varphi_1)$,
$a_{\mathrm{dG}}(v_{\mathrm{dG}},\varphi_2) - b_{\mathrm{dG}}(u_{\mathrm{dG}}, u_{\mathrm{dG}}, \varphi_2) = 0$.
The combined vector form seeks $\Psi_{\mathrm{dG}} \equiv (u_{\mathrm{dG}}, v_{\mathrm{dG}}) \in \boldsymbol{P}_2(\mathcal{T})$ such that

$$N_h(\Psi_{\mathrm{dG}}; \Phi_{\mathrm{dG}}) := A_{\mathrm{dG}}(\Psi_{\mathrm{dG}}, \Phi_{\mathrm{dG}}) + B_{\mathrm{dG}}(\Psi_{\mathrm{dG}}, \Psi_{\mathrm{dG}}, \Phi_{\mathrm{dG}}) - L_{\mathrm{dG}}(\Phi_{\mathrm{dG}}) = 0, \tag{4}$$

where for all $\Xi_{\mathrm{dG}} = (\xi_1,\xi_2), \Theta_{\mathrm{dG}} = (\theta_1,\theta_2), \Phi_{\mathrm{dG}} = (\varphi_1,\varphi_2) \in \boldsymbol{P}_2(\mathcal{T})$, $L_{\mathrm{dG}}(\Phi_{\mathrm{dG}}) := l_{\mathrm{dG}}(\varphi_1)$, $A_{\mathrm{dG}}(\Theta_{\mathrm{dG}}, \Phi_{\mathrm{dG}}) := a_{\mathrm{dG}}(\theta_1,\varphi_1) + a_{\mathrm{dG}}(\theta_2,\varphi_2)$, $B_{\mathrm{dG}}(\Xi_{\mathrm{dG}}, \Theta_{\mathrm{dG}}, \Phi_{\mathrm{dG}}) := b_{\mathrm{dG}}(\xi_1,\theta_2,\varphi_1) + b_{\mathrm{dG}}(\xi_2,\theta_1,\varphi_1) - b_{\mathrm{dG}}(\xi_1,\theta_1,\varphi_2)$. For $\varphi \in H^2(\mathcal{T})$ and $\Phi = (\varphi_1,\varphi_2) \in H^2(\mathcal{T}) \times H^2(\mathcal{T})$, define the mesh dependent norms $|\!|\!|\Phi|\!|\!|_{\mathrm{dG}}^2 := \|\varphi_1\|_{\mathrm{dG}}^2 + \|\varphi_2\|_{\mathrm{dG}}^2$, where $\|\varphi\|_{\mathrm{dG}}^2 := |\varphi|_{H^2(\mathcal{T})}^2 + \sum_{E\in\mathcal{E}} \frac{\sigma_1}{h_E^3} \|[\varphi]_E\|_{L^2(E)}^2 + \sum_{E\in\mathcal{E}} \frac{\sigma_2}{h_E} \|[\nabla\varphi\cdot\nu_E]_E\|_{L^2(E)}^2$.

Theorem 1 (Discrete inf-sup condition)**.** [3] *Let $\Psi \in \boldsymbol{H}^{2+\alpha}(\Omega) \cap \boldsymbol{X}$ be a regular solution to* (3)*. For sufficiently large σ_2 and sufficiently small h,*

$$0 < \widehat{\beta} \leq \inf_{\substack{\Theta_{\mathrm{dG}}\in\boldsymbol{P}_2(\mathcal{T}) \\ |\!|\!|\Theta_{\mathrm{dG}}|\!|\!|_{\mathrm{dG}}=1}} \sup_{\substack{\Phi_{\mathrm{dG}}\in\boldsymbol{P}_2(\mathcal{T}) \\ |\!|\!|\Phi_{\mathrm{dG}}|\!|\!|_{\mathrm{dG}}=1}} \Big(A_{\mathrm{dG}}(\Theta_{\mathrm{dG}}, \Phi_{\mathrm{dG}}) + 2B_{\mathrm{dG}}(\Psi, \Theta_{\mathrm{dG}}, \Phi_{\mathrm{dG}})\Big).$$

Moreover, for a suitably chosen interpolant of Ψ denoted as $\Pi_h\Psi$, the perturbed bilinear form $\tilde{\mathcal{A}}_{\mathrm{dG}}(\Theta_{\mathrm{dG}}, \Phi_{\mathrm{dG}}) := A_{\mathrm{dG}}(\Theta_{\mathrm{dG}}, \Phi_{\mathrm{dG}}) + 2B_{\mathrm{dG}}(\Pi_h\Psi, \Theta_{\mathrm{dG}}, \Phi_{\mathrm{dG}})$ also satisfies the discrete inf-sup condition.

For any $\Theta_{\mathrm{dG}} \in \boldsymbol{P}_2(\mathcal{T})$, let $\mu(\Theta_{\mathrm{dG}}) \in \boldsymbol{P}_2(\mathcal{T})$ solve $\tilde{\mathcal{A}}_{\mathrm{dG}}(\mu(\Theta_{\mathrm{dG}}), \Phi_{\mathrm{dG}}) = L_{\mathrm{dG}}(\Phi_{\mathrm{dG}}) + 2B_{\mathrm{dG}}(\Pi_h\Psi, \Theta_{\mathrm{dG}}, \Phi_{\mathrm{dG}}) - B_{\mathrm{dG}}(\Theta_{\mathrm{dG}}, \Theta_{\mathrm{dG}}, \Phi_{\mathrm{dG}})$ for all $\Phi_{\mathrm{dG}} \in \boldsymbol{P}_2(\mathcal{T})$. Then μ is well-defined, continuous and any fixed point of μ is a solution to (4) and vice-versa.

Theorem 2 (Existence, uniqueness and error estimates)**.** [3] *For sufficiently large σ_2 and sufficiently small h, there exists a unique solution Ψ_{dG} to the discrete problem* (4) *in a ball centered at $\Pi_h\Psi$ and radius Ch^α, where the constant $C \approx 1$ and $\alpha \in (1/2, 1]$ is the elliptic regularity index. Further, $|\!|\!|\Psi - \Psi_{\mathrm{dG}}|\!|\!|_{\mathrm{dG}} \leq Ch^\alpha$.*

The analysis extends to a C^0 interior penalty method for the von Kármán equations formally for $\sigma_1 \to \infty$ when σ_1 disappears but the trial and test functions become continuous. This scheme is the above dG method but with ansatz test

function restricted to globally continuous piecewise quadratic polynomials and excludes σ_1 term. For details of numerical results, see [3].

References

[1] Mallik, G. and Nataraj, N., *A nonconforming finite element approximation for the Von Kármán Equations*, ESAIM Math. Model. Numer. Anal. , **50** (2016), 433-454.
[2] Brenner, S. C. and Neilan, M. and Reiser, A. and Sung, L.-Y., *A C^0 interior penalty method for a von Kármán plate*, Numer. Math. , (2016), 1–30.
[3] Carstensen, C., Mallik, G. and Nataraj, N., *A priori and a posteriori error control of discontinuous Galerkin finite element methods for the von Kármán equations*, IMA J. Numer. Anal., *To appear.*

Optimal design of thin film solar cells

Peter Monk

We describe an ongoing project to develop a flexible and rigorously justified software tool for optimizing the design of thin film solar cells [1]. We use the differential evolution algorithm (DEA) [2] to optimize the material parameters (such as bandgap) and the geometry of the solar cell (for example, layer thicknesses and surface shapes) to maximize the efficiency of the solar cell. DEA is a derivative free optimization scheme, but requires many evaluations of the cost function (in this case the efficiency). This implies the need for fast simulation of a given design.

There are two steps to evaluate the efficiency of a solar cell:

Photonic model: Maxwell's equations need to be solved in the solar cell to find the generation rate of electrons and holes (this is proportional to the square of the magnitude of the electric field). We restrict ourselves to the case when the thin film solar cell is translation invariant in one direction, in which case Maxwell's equations decouples into s-polarized and p-polarized waves that satisfy different Helmholtz equations.

To solve the Helmholtz equations we use the Rigorous Coupled Wave Analysis (RCWA) method [3]. This is based on using Fourier series in the horizontal (periodic) direction, and a special linear algebra solver that results in a very rapid prediction of the electromagnetic field. Since the technique is meshless, it is easy to change both the geometry of the device and the material parameters for each simulation.

Unfortunately the method is not proven to converge, but numerical tests show quadratic convergence in the Fourier parameter for s-polarized waves, and much slower convergence for p-polarized waves ($O(N^{-1/3})$ where N is the highest order of the Fourier mode retained in the calculation).

Electron transport: We use the drift-diffusion model to simulate electron transport in the semiconductor layers of the device. This model involves the density of electrons and holes in the device as well as the static electric field generated by these entities. Diffusion dominated and transport dominated processes occur in the same simulation. We average the generation function produced by the photonic model, and use a the drift diffusion

system in one spatial dimension to simulate the device. Using the Hybridizable Discontinuous Galerkin (HDG) scheme [4], we can discretize the system using p-degree polynomials for each unknown in the system. The resulting system of nonlinear equations is solved by Newton's method, and by using different biasing voltages the optimal efficiency for a given design can be computed. This is employed by the DEA.

Computationally we observe non optimal $O(h^{p-1})$ order convergence. This is likely due to using equal degree polynomials for each unknown in the drift -diffusion system. Use of better balanced spaces will be investigated in the future.

We have used the above algorithm to optimize a representative solar cell. Future work will include investigating more novel designs, and implementing a full two dimensional drift diffusion mode.

References

[1] T. H. Anderson, B Civiletti, P. Monk, and A. Lakhtakia, "Combined Optoelectronic Simulation and Optimization of Solar Cells," in preparation (2018).

[2] R. Storn and K. Price, "Differential Evolution - a simple and efficient heuristic for global optimization over continuous spaces," *Journal of Global Optimization* **11**, pp. 341 – 359, 1997.

[3] J. Polo Jr., T. Mackay, and A. Lakhtakia, *Electromagnetic Surface Waves: A Modern Perspective*, Elsevier, Waltham, MA, USA, 2013.

[4] G. Fu, W. Qiu, and W. Zhang, "An analysis of HDG methods for convection-dominated diffusion problems," *ESAIM: Math. Model. Numer. Anal.* **49**, pp. 225–256, 2015.

A new framework for large strain electromechanics based on Convex Multi-Variable (CMV) strain energies

Antonio J. Gil

(joint work with Rogelio Ortigosa, Roman Poya)

Dielectric Elastomers (DE) are a class of Electro Active Polymers with outstanding actuation properties. Voltage induced area expansions of 1980% on a DE membrane have been recently reported. In this case, the electromechanical instability is harnessed as a means for obtaining these electrically induced massive deformations with potential applications in soft robots. Computational simulation in this context becomes extremely challenging and must be addressed *ab initio* by the definition of well-posed constitutive models.

In this presentation, we postulate a new Convex Multi-Variable (CMV) variational framework for the analysis of these materials exhibiting massive deformations [2, 3, 4]. This extends the concept of polyconvexity [1] to strain energies which depend on non-strain based variables introducing other physical measures such as the electric displacement. A new definition of the electro-mechanical internal energy is introduced, being expressed as a Convex Multi-Variable (CMV) function of a new extended set of electromechanical arguments. Crucially, this

new definition of the internal energy enables the most accepted constitutive inequality, namely ellipticity, to be extended to the entire range of deformations and electric fields and, in addition, to incorporate the electromechanical energy of the vacuum, and hence that for ideal dielectric elastomers, as a degenerate case. Spurious numerical instabilities can then effectively be removed from the model whilst maintaining real physical instabilities. Hyperbolicity, variational principles and Finite Element functional spaces will be shown prior to demonstrating the potential of the new paradigm through extremely challenging numerical examples involving wrinkling and the onset of instabilities [5, 6].

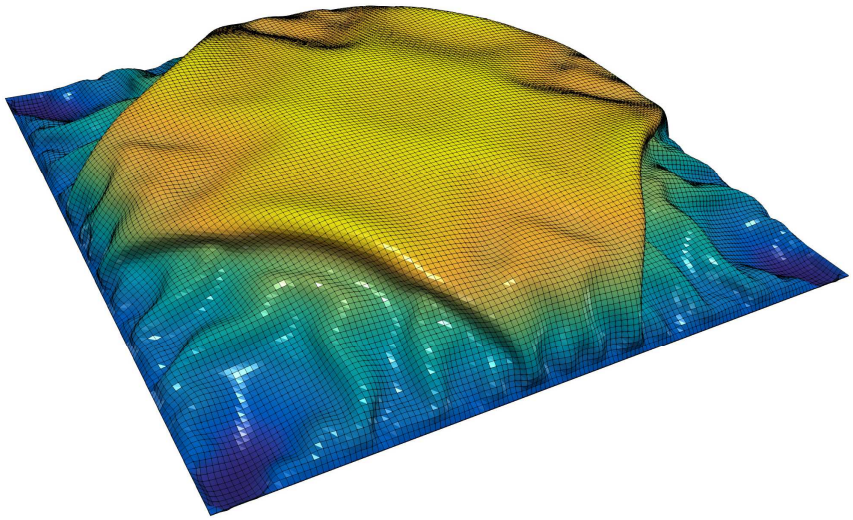

FIGURE 1. Dielectric elastomer undergoing massive deformations

REFERENCES

[1] J.M. Ball, *Convexity conditions and existence theorems in nonlinear elasticity*, Archive for Rational Mechanics and Analysis **63** (1976), 337–403.

[2] A.J. Gil, R. Ortigosa, *A new framework for large strain electromechanics based on convex multi-variable strain energies: Variational formulation and material characterisation*, Computer Methods in Applied Mechanics and Engineering **302** (2016), 293–328.

[3] R. Ortigosa, A.J. Gil, *A new framework for large strain electromechanics based on convex multi-variable strain energies: Finite Element discretisation and computational implementation*, Computer Methods in Applied Mechanics and Engineering **302** (2016), 329–360.

[4] R. Ortigosa, A.J. Gil, *A new framework for large strain electromechanics based on convex multi-variable strain energies: Conservation laws, hyperbolicity and extension to electromagnetomechanics*, Computer Methods in Applied Mechanics and Engineering **309** (2016), 202–242.

[5] R. Poya, A.J. Gil, R. Ortigosa, *A high performance data parallel tensor contraction framework: Application to coupled electro-mechanics*, Computer Physics Communications **216** (2017), 35–52.

[6] R. Poya, A.J. Gil, R. Ortigosa, R. Sevilla, J. Bonet, W. Wall, *A curvilinear high order finite element framework for electromechanics: from linearised electro-elasticity to massively deformable dielectric elastomers*, Computer Methods in Applied Mechanics and Engineering **329** (2018), 75–117.

The DPG* Method

Brendan Keith
(joint work with Leszek Demkowicz, Jay Gopalakrishnan)

We present a novel framework for the construction and analysis of finite element methods with trial and test spaces of unequal dimension. At the heart of this work is a new duality theory suitable for variational formulations with non-symmetric functional settings [5]. The primary application of this theory, in this talk, is the development and analysis of discontinuous PetrovGalerkin (DPG) finite element methods; in particular, goal-oriented adaptive mesh refinement strategies therein.

We introduce the DPG* finite element method [3]: the dual to the DPG method. DPG, as a methodology, can be viewed as a practical means to solve overdetermined discretizations of boundary value problems. In a similar way, DPG* delivers a methodology for underdetermined discretizations. Supporting this new finite element method are new results on a priori error estimation and a posteriori error control. Notably, it is demonstrated that the convergence of a DPG* method is controlled, in part, by a Lagrange multiplier variable which plays the role of the solution variable in DPG methods. The presented theory is applied to two representative problems coming from linear and nonlinear partial differential equation models. To facilitate a thorough mathematical analysis, Poisson's equation is considered. To demonstrate the utility of the approach in less tractable scenarios, the Oldroyd-B fluid model is also considered. Taken together, the combined analysis of these two models effectively demonstrates the utility of the newly developed paradigm. Taken together, the combined analysis of these two models effectively demonstrates the utility of the newly developed paradigm. This talk is largely based on Keith's Ph.D. dissertation [2].

References

[1] L. Demkowicz, J. Gopalakrishnan, B. Keith, *The DPG-star method*, arXiv:1809.03153 [math.NA].

[2] B. Keith, *New ideas in adjoint methods for PDEs: A saddle-point paradigm for finite element analysis and its role in the DPG methodology*, PhD thesis, The University of Texas at Austin, Austin, Texas, U.S.A., 2018

[3] B. Keith, L. Demkowicz, J. Gopalakrishnan, *DPG* method*, ICES Report 17-25, The University of Texas at Austin, 2017.

[4] B. Keith, P. Knechtges, N.V. Roberts, S. Elgeti, M. Behr, L. Demkowicz, *An ultraweak DPG method for viscoelastic fluids*, Journal of Non-Newtonian Fluid Mechanics **247** (2017), 107–122.

[5] B. Keith, A. Vaziri Astaneh, L. Demkowicz, *Goal-oriented adaptive mesh refinement for non-symmetric functional settings*, arXiv:1711.01996 [math.NA].

A cut finite element method for incompressible two-phase Navier-Stokes flows

Sara Zahedi
(joint work with Thomas Frachon)

We develop a space-time Cut Finite Element Method (CutFEM) for the time-dependent Navier-Stokes equations involving two immiscible incompressible fluids with different viscosities, densities, and with surface tension [1]. Due to surface tension effects at the interface separating the two fluids and different fluid viscosities the pressure may be discontinuous and the velocity field may have a kink across the interface. In order to accurately capture these discontinuities across evolving interfaces we build the solution during a time interval from two solutions, one on each side of the interface with overlap on the elements cut by the interface during the time interval, see Figure 1. Physical interface conditions such as the jump in the normal stress are imposed weakly and glue the two solutions on the interface [2]. We use a space-time strategy with discontinuous elements in time and continuous elements in space. The cut finite element method allows the interface to be arbitrarily located with respect to a fixed background mesh. Stabilization terms which ensure well-posedness of the resulting algebraic system of equations, independently of how the interface cuts through the fixed mesh, without destroying the optimal convergence order of the method are added to the variational formulation. These stabilization terms also ensure good stability properties and allow us to approximate space-time integrals using quadrature rules in time. Our method has a convenient implementation as it does not reconstruct the space-time domain but rather directly uses quadrature rules to approximate the space-time integrals in the variational formulation [3, 4]. The time discretization given by our method is closely related to implicit finite difference methods. The backward Euler discretization can for example be obtained by using piecewise constant functions in time.

We also present an accurate method for the surface tension force based on the computation of a stabilized mean curvature vector. By stabilizing the L^2 projection in the computation of the mean curvature vector with an appropriate stabilization term we gain one order in the convergence in the L^2-norm. In [5] we prove this result for linear elements. For a stabilization term that can be used both with linear as well as higher order elements see [4, 6].

We present a space-time cut finite element method which is able to accurately capture both the strong discontinuity in the pressure and the weak discontinuity in the velocity field across moving interfaces without conforming the mesh to these interfaces or regularizing the problem.

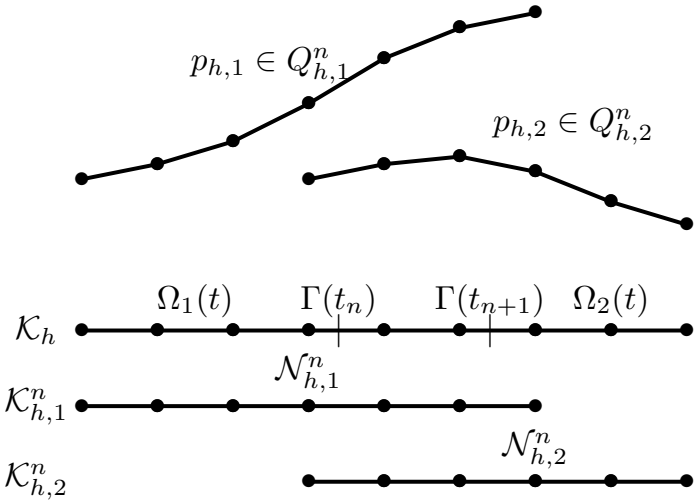

FIGURE 1. Illustration of the mesh and the pressure space associated with a time interval $I_n = (t_n, t_{n+1}]$ in a one space dimensional model. The interface evolves from $\Gamma(t_n)$ to $\Gamma(t_{n+1})$ during the time interval I_n.

REFERENCES

[1] T. Frachon, S. Zahedi, *A cut finite element method for incompressible two-phase Navier-Stokes flows*, arXiv:1808.02662.

[2] P. Hansbo, M. G. Larson, S. Zahedi, *A cut finite element method for a Stokes interface problem*, Appl. Numer. Math. **85** (2014) 90–114.

[3] P. Hansbo, M. G. Larson, S. Zahedi, *A cut finite element method for coupled bulk-surface problems on time-dependent domains*, Comput. Methods Appl. Mech. Engrg. **307** (2016) 96–116.

[4] S. Zahedi, *A space-time cut finite element method with quadrature in time*, in: Geometrically Unfitted Finite Element Methods and Applications, Lecture Notes in Computational Science and Engineering, Springer, 2018, pp. 281–306.

[5] P. Hansbo, M. G. Larson, S. Zahedi, *Stabilized finite element approximation of the mean curvature vector on closed surfaces*, SIAM J. Numer. Anal. **53** (4) (2015) 1806–1832.

[6] M. G. Larson, S. Zahedi, *Stabilization of high order cut finite element methods on surfaces*, arXiv:1710.03343.

Optimal Convergence Rates of dPG

FRIEDERIKE HELLWIG

(joint work with Carsten Carstensen)

The discontinuous Petrov-Galerkin methodology enjoys a built-in a posteriori error control [1] in some computable residual term plus data approximation terms. This talk establishes an alternative error estimator [2], which is globally equivalent, but allows for the proof of the axioms of adaptivity and so guarantees optimal convergence rates of the associated adaptive algorithm. The talk exemplifies the analysis for the Poisson model problem $-\Delta u = f$ with a right-hand side $f \in L^2(\Omega)$ in the polyhedral domain Ω simultaneously for the four lowest-order discontinuous

Petrov-Galerkin schemes as a generalization of an approach for a lowest-order primal dPG method for a nonlinear problem [3]. Those are rewritten in terms of the first-order nonconforming Crouzeix-Raviart functions $CR^1_0(\mathcal{T})$ and its conforming subspace $S^1_0(\mathcal{T})$, with respect to a shape-regular triangulation $\mathcal{T}$ into simplices, some projection $Q : L^2(\Omega) \to L^2(\Omega)$ and a parameter α. For solutions $(v_{CR}, u_C) \in CR^1_0(\mathcal{T}) \times S^1_0(\mathcal{T})$ to this reduced mixed system, the novel error estimator $\eta(T)$ consists of the expected volume contributions $|T|^{1/n}\|f - \alpha Q v_{CR}\|_{L^2(T)}$ and the jump terms of the piecewise gradient of v_{CR} across the sides of any simplex $T \in \mathcal{T}$. The estimator exclusively involves the variable v_{CR} and seemingly ignores the conforming contribution u_C, but surprisingly also controls the error term $u - u_C$. The optimal convergence rates rely on standard arguments for stability and reduction, while the discrete reliability involves an additional term $h_0\eta(\widehat{\mathcal{T}})$ for an admissible refinement $\widehat{\mathcal{T}}$ of $\mathcal{T}$; this eventually enforces the additional condition of a sufficiently small initial mesh-size h_0 for optimal convergence rates within the abstract framework of [4].

References

[1] C. Carstensen, L. Demkowicz and J. Gopalakrishnan, *A posteriori error control for DPG methods*, SIAM J. Numer. Anal. **52**(3) (2014), 1335–1353.

[2] C. Carstensen and F. Hellwig, *Optimal convergence rates for adaptive lowest-order discontinuous Petrov-Galerkin schemes*, SIAM J. Numer. Anal. **56**(2) (2018), 1091–1111.

[3] C. Carstensen, P. Bringmann, F. Hellwig and P. Wriggers, *Nonlinear discontinuous Petrov-Galerkin methods*, Numer. Math. **139**(3) (2018), 529–561.

[4] C. Carstensen and H. Rabus, *Axioms of adaptivity with separate marking for data resolution*, SIAM J. Numer. Anal. **55**(6) (2017), 2644–2665.

Staggered discontinuous Galerkin methods on general meshes

Eun-Jae Park

(joint work with Zhao, Lina)

In this report, we propose and analyze a locally conservative, lowest order staggered discontinuous Galerkin (SDG) method of minimal dimension on general quadrilateral/polygonal meshes for elliptic problems [5]. We define the lowest order SDG method by connecting the center point of a certain quadrilateral/polygon (primal mesh) to all the vertices, then the primal mesh is divided into the union of triangles, which are the primal submeshes (see Figure 1 for an illustration). Then we can define two piecewise constant finite element spaces earning continuity over different edges to approximate the potential u and the vector variable $\boldsymbol{p}$, namely, the potential is continuous over the primal edges, and the vector variable is continuous over the dual edges. The staggered continuity property recasts the proposed method to be locally conservative. Since the finite element functions are composed of piecewise constant functions, the implementation is particularly simple without complex integrations on the mesh, and affine mapping is not needed. If the quadrilateral is reduced to a square, then the mass matrix for the vector variable becomes just a diagonal matrix. In addition, our method can be flexibly

applied to highly distorted grids. Moreover, hanging nodes are allowed, which can be simply treated as additional vertices. A priori error analysis covering low regularity can be stated in the theorem below.

Theorem 1. *Assume that* $(\boldsymbol{p}, u) \in (H^{\epsilon}(\Omega)^2 \cap H(\mathrm{div}, \Omega)) \times H^{1+\epsilon}(\Omega), 0 < \epsilon \leq 1$. *Here,* H^m *is the standard Sobolev space. Let* $(\boldsymbol{p}_h, u_h)$ *be the numerical solution obtained from the lowest order SDG method, then there exists a positive constant* C *such that*

$$\|u - u_h\|_0 \leq C(h^{\min\{1,2\epsilon\}}\|u\|_{1+\epsilon,\Omega} + (\sum_{\tau \in \mathcal{T}_h} h_\tau^2 \|f\|_{0,\tau}^2)^{1/2}),$$

$$\|\boldsymbol{p} - \boldsymbol{p}_h\|_0 \leq C h^{\epsilon}\|u\|_{1+\epsilon,\Omega}.$$

On the other hand, adaptive mesh refinement is an attractive tool for general meshes due to their flexibility and simplicity in handling hanging nodes. We develop a reliable and efficient error estimator for the lowest order SDG method on general quadrilateral and polygonal meshes. Notice that the potential arising from numerical approximation is defined as a piecewise constant function over the domain, it is impossible to measure the error estimator in the energy norm of potential unless postprocessing is involved. Therefore, we design a residual based error estimator on the L^2 error in vector variable. In order to achieve this, the main ingredient is the Helmholtz decomposition for the vector variable error (cf. [1, 4]). Combining this with the standard interpolation theory, we can achieve the residual based error estimator. Numerical results indicate that optimal convergence can be achieved for both the potential and vector variables even for highly distorted grids, and the singularity can be well-captured by the proposed error estimator.

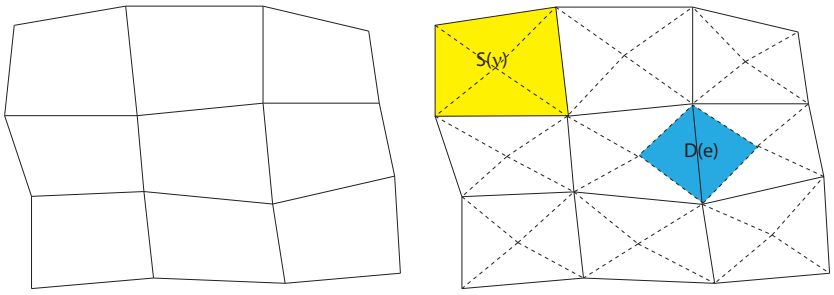

FIGURE 1. Schematic of primal mesh $S(\nu)$, dual mesh $D(e)$ and primal submesh (triangulations).

REFERENCES

[1] A. Alonso, *Error estimators for a mixed method*, Numer. Math., **74** (1996), 385–395.

[2] T. Arbogast and M. R. Correa, *Two families of* $H(div)$ *mixed finite elements on quadrilaterals of minimal dimension*, SIAM J. Numer. Anal., **54** (2016), 3332–3356.

[3] L. Beirão da Veiga, F. Brezzi, A. Cangiani, G. Manzini, L.D. Marini, and A. Russo, *Basic principles of virtual element method*, Math. Models Methods Appl. Sci., **23** (2013), 199–214.

[4] C. Carstensen, *A posteriori error estimate for the mixed finite element method*, Math. Comp., **66** (1997), 465–476.
[5] L. Zhao and E.-J. Park, *A staggered discontinuous Galerkin method of minimal dimension on quadrilateral and polygonal meshes*, SIAM J. Sci. Comput., **40** (2018), 2543–2567.

Heterogeneous Asynchronous time integrators for transient dynamics co-simulations

Anthony Gravouil
(joint work with University of Lyon, INSA-Lyon, LaMCoS, CNRS, France)

In non-smooth transient structural dynamics, the choice of the time step and the time integrator has a critical impact on the feasibility of the simulation. For instance, during an earthquake, a bridge crane, usually located overhead in buildings, may be subjected to multiple impacts between crane wheels and rail. These multiple impacts cause significant damage in the structure. Then the qualification of these structures with respect to normative seismic design requirements, which are continuously developing and becoming more and more stringent, requires strengthened simulation techniques especially to model the impact phenomenon. Furthermore, multiple time-scales coexist in a bridge crane under seismic loading. In that case, the use of multi-time scale methods is suitable. Here, we propose a new explicit-implicit heterogeneous asynchronous time integrator (HATI) for non-smooth transient dynamics with possible contacts and impacts. In a first step we introduce a Moreau-based event-capturing explicit time integrator for contact/impact problems. In a second step, a two time scales explicit-implicit HATI is developed: it consists in using an explicit time integrator with a fine time scale in the contact area, while an implicit time integrator is adopted in the other parts in order to capture the low frequency content of the solution and to optimize the CPU time. 3D Transient dynamics applications illustrate the robustness and the efficiency of the proposed approach.

References

[1] F. Fekak, M. Brun, A. Gravouil, B. Depale, *A new heterogeneous asynchronous explicit-implicit time integrator for nonsmooth dynamics*, Computational Mechanics **50** (2017), 199–225.
[2] A. Gravouil, A. Combescure, M. Brun, *Heterogeneous asynchronous time integrators for computational structural dynamics*, International Journal for Numerical Methods in Engineering **102** (2015), 202–232.
[3] V. Acary, *Energy conservation and dissipation properties of time-integration methods for non smooth elastodynamics with contact*, ZAMM-Journal of Applied Mathematics and Mechanics **96** (2016), 585–603.
[4] A. Lew, J. Marsden, M. Ortiz, M. West, *Variational time integrators*, International Journal for Numerical Methods in Engineering **60** (2004), 153–212.
[5] M. Jean, *The non-smooth contact dynamics method*, Computer methods in applied mechanics and engineering **177** (1999), 235–257.
[6] T.A. Laursen, *Computational Contact and Impact Mechanics: Fundamentals of Modeling Interfacial Phenomena in Nonlinear Finite Element Analysis*, Springer Science and Business Media (2002).

[7] F. Armero, E. Petocz, *Formulation and analysis of conserving algorithms for frictionless dynamic contact/impact problems*, Computer methods in applied mechanics and engineering **158** (1998), 269–300.
[8] P. Alart, A. Curnier, *A mixed formulation for frictional contact problems prone to Newton like solution methods*, Computer methods in applied mechanics and engineering **92** (1991), 353–375.
[9] T. Belytschko, M. Neal, *Contact-impact by the pinball algorithm with penalty and Lagrangian methods*, International Journal for Numerical Methods in Engineering **31** (1991), 547–572.

Application of assumed stress finite elements in hyperelasticity

Nils Viebahn
(joint work with Jörg Schröder, Peter Wriggers)

We discuss here an idea for the extension of an assumed stress element, see [1, 2], to the hyperelastic framework. The crucial point is an implicit solution procedure for the constitutive relation, based on a general free energy function ψ. The strong form of the considered problem can be written as:

Seek the displacement $\boldsymbol{u}$ and the second Piola-Kirchhoff stresses $\boldsymbol{S}$ such that

$$
\begin{aligned}
-\mathrm{Div}[\boldsymbol{F}\boldsymbol{S}] &= \boldsymbol{0} && \text{on } \mathcal{B},\\
\boldsymbol{E} &= \partial_S \chi(\boldsymbol{S}) && \text{on } \mathcal{B},\\
\boldsymbol{u} &= \overline{\boldsymbol{u}}_D && \text{on } \partial\mathcal{B}_D,\\
(\boldsymbol{F}\boldsymbol{S})\cdot\boldsymbol{N} &= \overline{\boldsymbol{t}}_N && \text{on } \partial\mathcal{B}_N,
\end{aligned}
\tag{1}
$$

with $\boldsymbol{F} = \boldsymbol{I} + \mathrm{Grad}\boldsymbol{u}$, $\boldsymbol{E} = \frac{1}{2}(\boldsymbol{C} - \boldsymbol{I})$, $\boldsymbol{C} = \boldsymbol{F}^T\boldsymbol{F}$, the complementary stored energy $\chi(\boldsymbol{S})$ and boundary values $\overline{\boldsymbol{u}}_D$, $\overline{\boldsymbol{t}}_N$. The major problem in this formulation is, that the complementary stored energy function is only defined explicitly for special cases.In our approach, we will calculate its dependencies implicitly in each load step, introducing an internal variable $\boldsymbol{E}^c$ which satisfies the constitutive relation

$$
\boldsymbol{r}(\boldsymbol{E}^c) = \boldsymbol{S} - \partial_E(\psi(\boldsymbol{E}))|_{\boldsymbol{E}=\boldsymbol{E}^c} = \boldsymbol{0}\,. \tag{2}
$$

Substitution of $\partial_S\chi(\boldsymbol{S})$ with $\boldsymbol{E}^c$ leads after integration by parts to the weak forms

$$
\begin{aligned}
G_u &= \int_{\mathcal{B}} \delta\boldsymbol{E} : \boldsymbol{S}\,\mathrm{d}V - \int_{\partial\mathcal{B}_N} \delta\boldsymbol{u}\cdot\overline{\boldsymbol{t}}_N\,\mathrm{d}A = 0\\
G_S &= \int_{\mathcal{B}} \delta\boldsymbol{S} : (\boldsymbol{E} - \boldsymbol{E}^c)\,\mathrm{d}V = 0 \quad \text{with } \boldsymbol{E}^c = \partial_S\chi(\boldsymbol{S})
\end{aligned}
\tag{3}
$$

and corresponding linearizations as

$$
\Delta G_u = \int_{\mathcal{B}} (\Delta\delta\boldsymbol{E} : \boldsymbol{S} + \delta\boldsymbol{E} : \Delta\boldsymbol{S})\,\mathrm{d}V\,, \quad \Delta G_S = \int_{\mathcal{B}} \delta\boldsymbol{S} : (\Delta\boldsymbol{E} - \Delta\boldsymbol{E}^c)\,\mathrm{d}V \tag{4}
$$

with the internal relationship $\Delta\boldsymbol{E}^c = \left(\left(\dfrac{\partial^2\psi(\boldsymbol{E})}{\partial\boldsymbol{E}\,\partial\boldsymbol{E}}\right)\Big|_{\boldsymbol{E}=\boldsymbol{E}^c}\right)^{-1} : \Delta\boldsymbol{S}$. Discretization of the displacements with continuous piecewise bilinear interpolation functions

and a five parameter mode for the second Piola-Kirchhoff stress

$$\underline{\boldsymbol{u}} = \underline{\boldsymbol{N}}\,\underline{\boldsymbol{d}}\,, \quad \underline{\boldsymbol{S}} = \begin{pmatrix} S_{11} \\ S_{22} \\ S_{12} \end{pmatrix} = \underline{\mathbb{L}}\,\underline{\boldsymbol{\beta}} = \begin{pmatrix} 1 & 0 & 0 & \eta & \frac{a_2^2}{b_2^2}\xi \\ 0 & 1 & 0 & \frac{b_1^2}{a_1^2}\eta & \xi \\ 0 & 0 & 1 & \frac{b_1}{a_1}\eta & \frac{a_2}{b_2}\xi \end{pmatrix} \begin{pmatrix} \beta_1 \\ \beta_2 \\ \beta_3 \\ \beta_4 \\ \beta_5 \end{pmatrix} \tag{5}$$

where the parameter a_i and b_j are depending on the nodal coordinates as

$$\begin{pmatrix} a_1 & b_1 \\ a_2 & b_2 \end{pmatrix} = \frac{1}{4} \begin{pmatrix} -1 & 1 & 1 & -1 \\ -1 & -1 & 1 & 1 \end{pmatrix} \begin{pmatrix} x_1 & y_1 \\ x_2 & y_2 \\ x_3 & y_3 \\ x_4 & y_4 \end{pmatrix} . \tag{6}$$

This leads to the incremental system of equations as

$$\mathrm{Lin}G = \begin{bmatrix} \delta\underline{\boldsymbol{d}}^T \\ \delta\underline{\boldsymbol{\beta}}^T \end{bmatrix} \left(\begin{bmatrix} \underline{\boldsymbol{K}}_{uu} & \underline{\boldsymbol{K}}_{u\sigma}{}^T \\ \underline{\boldsymbol{K}}_{u\sigma} & \underline{\boldsymbol{K}}_{\sigma\sigma} \end{bmatrix} \begin{bmatrix} \Delta\underline{\boldsymbol{d}} \\ \Delta\underline{\boldsymbol{\beta}} \end{bmatrix} + \begin{bmatrix} \underline{\boldsymbol{r}}_u \\ \underline{\boldsymbol{r}}_\sigma \end{bmatrix} \right) = 0\,. \tag{7}$$

For a typical element e the system matrices are be given by

$$\begin{aligned} &\underline{\boldsymbol{K}}^e_{uu} := \int_{\mathcal{B}^e} \underline{\boldsymbol{\Xi}}\,\underline{\boldsymbol{S}}\,\mathrm{d}V\,, \quad \underline{\boldsymbol{K}}^e_{u\sigma} := \int_{\mathcal{B}^e} \underline{\mathbb{L}}^T\underline{\boldsymbol{B}}\,\mathrm{d}V\,, \quad \underline{\boldsymbol{K}}^e_{\sigma\sigma} := \int_{\mathcal{B}^e} \underline{\mathbb{L}}^T\underline{\mathbb{D}}\,\underline{\mathbb{L}}\,\mathrm{d}V\,, \\ &\underline{\boldsymbol{r}}^e_u := \int_{\mathcal{B}^e} \underline{\boldsymbol{B}}^T\underline{\boldsymbol{S}}\,\mathrm{d}V - \int_{\partial\mathcal{B}^e_N} \underline{\boldsymbol{N}}^T\underline{\bar{\boldsymbol{t}}}\,\mathrm{d}A\,, \quad \underline{\boldsymbol{r}}^e_\sigma := \int_{\mathcal{B}^e} \underline{\mathbb{L}}^T(\underline{\boldsymbol{E}} - \underline{\boldsymbol{E}}^c)\,\mathrm{d}V\,, \end{aligned} \tag{8}$$

where $\underline{\boldsymbol{B}}$ is a suitable matrix containing the spatial derivatives of $\underline{\boldsymbol{N}}$, $\underline{\boldsymbol{\Xi}}$ is defined by $\Delta\underline{\boldsymbol{B}} = \underline{\boldsymbol{\Xi}}\Delta\underline{\boldsymbol{d}}$ and $\underline{\mathbb{D}}$ is the compliance matrix $\left(\left(\frac{\partial^2\psi(\boldsymbol{E})}{\partial\boldsymbol{E}\,\partial\boldsymbol{E}} \right) \big|_{\boldsymbol{E}=\boldsymbol{E}^c} \right)^{-1}$. A numerical example depicts the potential of the proposed formulation. We consider the Cook's membrane problem, depicted in Figure 1 with nearly incompressible material (Young's modulus $E = 200$ and Poisson's ratio $\nu = 0.4999$) considering

$$\psi = \frac{\Lambda}{4}(\det\boldsymbol{F}^2 - 1) - (\frac{\Lambda}{2} + \mu) + \ln[\det\boldsymbol{F}] + \frac{\mu}{2}(\mathrm{tr}\boldsymbol{C} - 3)\,. \tag{9}$$

Figure 1 depicts the mesh convergence of the tip displacement at the upper right

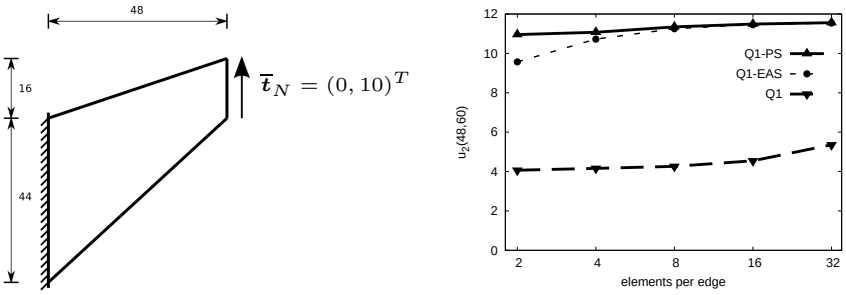

FIGURE 1. Numerical Benchmark of the Cook's membrane

node. It can be seen that the proposed formulation performs extraordinary good. Furthermore, only a single load step was necessary in order to apply the complete

deformation, whereas the EAS formulation requires more lode steps. Unfortunately, the proposed element suffers due to nonphysical hourglassing modes. A deeper understanding of the underlying causes for these additional modes and the development of possible treatments are subjects of ongoing research.

References

[1] T.H.H. Pian and K. Sumihara, IJNME, **20** (1984), 1685–1695.
[2] G. Yu, X. Xie and C. Carstensen, CMAME, **200** (2011), 2421–2433.

Partial Relaxation of Vertex Continuity of Nonnested (Conforming) Methods

Jun Hu
(joint work with Carsten Carstensen, Rui Ma)

The problems that are most frequently solved in scientific and engineering computing may probably be the elasticity equations. The finite element method (FEM) was invented in analyzing the stress of the elastic structures in the 1950s. The mixed FEM within the Hellinger-Reissner (H-R) principle for elasticity yields a direct stress approximation since it takes both the stress and displacement as an independent variable; while the displacement FEM only gives an indirect stress approximation. However, the symmetry of the stress plus the stability conditions make the design of the mixed FEM for elasticity surprisingly hard, which has been regarded as a long standing open problem [3]. In 2002, using the elasticity complexes, Arnold and Winther designed the first family of symmetric mixed elements with polynomial shape functions on triangular grids in 2D [4] which was extended to tetrahedral grids in 3D [3] and to rectangular grids in 2D [2]. Recently, the author and his collaborators developed a new framework to design and analyze the mixed FEM of elasticity problems, which yields optimal symmetric mixed FEMs. In addition, those elements are very easy to implement since their basis functions, based on those of the scalar Lagrange elements, can been explicitly written down by hand. The main ingredients of this framework are a structure of the discrete stress space on both simplicial and product grids, two basic algebraic results, and a two-step stability analysis method, see more details in [7, 8, 10, 11, 12].

The $H(\mathrm{div})$ conformity of discrete stresses only requires the continuity of normal components of symmetric matrix-valued piecewise polynomials. However, due to the constraint of the symmetry, all the conforming mixed elements mentioned above impose the C^0 continuity of discrete stresses at vertices. This introduces some inconsistency errors when discretizing some interface problems and stress boundary condition problems. Besides, because of the C^0 continuity of discrete stresses at vertices, the stress space on the coarse mesh is not a subspace of that on the fine mesh, which causes the difficulty of the convergence analysis of adaptive algorithms for the aforementioned elements.

A similar situation happens for most of H^2 conforming elements of fourth order problems. In fact, one of the most popular conforming plate elements dates back

to Argyris [1] with a quintic polynomial space $P_5(T)$ on a triangle T and 21 linear functionals including the function value partial derivatives of order $0, 1, 2$ at each vertex and the normal derivative at the mid-point of each edge. Even if $\mathcal{T}_h$ is some refinement of $\mathcal{T}_H$, the coarser Argyris finite element space with respect to $\mathcal{T}_H$ is in general *not* a subspace of the finer Argyris finite element space with respect to $\mathcal{T}_h$. The reason is that the Argyris finite element functions are C^1 conforming, but their second derivative with respect to the normal direction is discontinuous at the midpoint of an edge. This non-nestedness of the Argyris finite element space under admissible refinement of the underlying triangulation leads to theoretical difficulties in multilevel schemes such as the adaptive mesh-refining and multigrid solver methodologies.

We present a universal way to partially relax nonnested conforming methods for partial differential equations. We apply it to Argyris element of fourth order problems and mixed finite elements of elasticity equations, which results in conforming nested methods. We design adaptive and V-cycle multigrid algorithms for these extended methods and prove their convergence and optimality. Finally we provide some numerical examples to illustrate the theoretical results.

References

[1] J. H. Argyris, I. Fried and D. W. Scharpf, The TUBA family of plate elements for the matrix displacement method, The Aeronautical Journal of the Royal Aeronautical Society 72 (1968), 514–517.

[2] D. N. Arnold and G. Awanou, Rectangular mixed finite elements for elasticity, Math. Models Methods Appl. Sci. 15 (2005), 1417–1429.

[3] D. Arnold, G. Awanou and R. Winther. Finite elements for symmetric tensors in three dimensions. Math. Comp. 77 (2008), 1229–1251.

[4] D. N. Arnold and R. Winther. Mixed finite element for elasticity. Numer. Math. 92 (2002), 401–419.

[5] L. Chen, J. Hu, and X. Huang. Fast auxiliary space preconditioner for linear elasticity in mixed form. Math. Comp. 87 (2018), 1601–1633.

[6] L. Chen, J. Hu, X. Huang and H. Man. Residual-based a posteriori error estimates for symmetric conforming mixed finite elements for linear elasticity problems. Sci. China Math. 61 (2018), 973–992.

[7] J. Hu. Finite element approximations of symmetric tensors on simplicial grids in $\mathbb{R}^n$: the higher order case. J. Comput. Math. 33 (2015), 283–296.

[8] J. Hu, A new family of efficient conforming mixed finite elements on both rectangular and cuboid meshes for linear elasticity in the symmetric formulation, SIAM J. Numer. Anal., 53(2015), pp. 14381463.

[9] J. Hu and G. Yu. A unified analysis of quasi-optimal convergence for adaptive mixed finite element methods. SIAM J. Numer. Anal. 56 (2018), 296–316.

[10] J. Hu and S. Zhang. A family of conforming mixed finite elements for linear elasticity on triangular grids. arXiv:1406.7457, 2014.

[11] J. Hu and S. Zhang. A family of symmetric mixed finite elements for linear elasticity on tetrahedral grids. Sci. China Math. 58 (2015), 297–307.

[12] J. Hu and S. Zhang. Finite element approximations of symmetric tensors on simplicial grids in $\mathbb{R}^n$: The lower order case. Math. Models Methods Appl. Sci. 26 (2016), 1649–1669.

Reporter: Friederike Hellwig